Somatotopic specificity of perceptual and neurophysiological changes associated with visuo-proprioceptive realignment

Jasmine L. Mirdamadi[1,2], Courtney R. Seigel[1], Stephen D. Husch[2], Hannah J. Block[1,2]

[1]Program in Neuroscience, Indiana University Bloomington

[2]Department of Kinesiology, School of Public Health, Indiana University Bloomington

Running title: Somatotopic specificity in realignment

Corresponding Author:

Dr. Hannah J. Block

hjblock@indiana.edu

812-855-5390

1025 E. 7th St. SPH 112

Bloomington, IN, 47405 USA

Abstract

When visual and proprioceptive estimates of hand position disagree (e.g., viewing the hand underwater), the brain realigns them to reduce mismatch. This perceptual change is reflected in primary motor cortex (M1) excitability, suggesting potential relevance for hand movement. Here we asked whether fingertip visuo-proprioceptive misalignment affects only the brain's representation of that finger (somatotopically focal), or extends to other parts of the limb that would be needed to move the misaligned finger (somatotopically broad). In Experiments 1 and 2, before and after misaligned or veridical visuo-proprioceptive training at the index finger, we used transcranial magnetic stimulation (TMS) to assess M1 representation of five hand and arm muscles. The index finger representation showed an association between M1 excitability and visuo-proprioceptive realignment, as did the pinkie finger representation to a lesser extent. Forearm flexors, forearm extensors, and biceps did not show any such relationship. In Experiment 3, participants indicated their proprioceptive estimate of the fingertip, knuckle, wrist, and elbow, before and after misalignment at the fingertip. Proprioceptive realignment at the knuckle, but not the wrist or elbow, was correlated with realignment at the fingertip. These results suggest the effects of visuo-proprioceptive mismatch are somatotopically focal in both sensory and motor domains.

Keywords: Proprioception, motor cortex, somatotopy, TMS

The brain normally has access to true hand position (Y) through vision and proprioception. The image of the hand on the retina provides a visual estimate ($\hat{Y}_V$), while receptors in the muscles and joints of the arm and hand provide a proprioceptive estimate ($\hat{Y}_P$). To form a single estimate with which to guide behavior, the brain is thought to weight and combine them into a single, integrated estimate of hand position (Ghahramani et al. 1997). If there is a spatial misalignment between modalities, as when the hand is submerged in water, which refracts light (Fig. 1A), the brain can realign one or both ($\Delta\hat{Y}_V$, $\Delta\hat{Y}_P$) to compensate (Block and Bastian 2011; Ghahramani et al. 1997). Such a change in multisensory perception presumably affects perceived hand position, and thus motor planning with that hand. However, multisensory and motor processing have traditionally been examined separately, limiting our understanding of how these systems interact.

In practice, creating a spatial mismatch between visual and proprioceptive estimates of hand position can elicit both motor and perceptual changes (Block and Bastian 2011; Rossi et al. 2021), depending on task parameters. Prism adaptation is a classic example: with the visual field shifted by prisms, an individual viewing their own hand experiences a visuo-proprioceptive mismatch. Moving the hand will likely result in systematic errors, which can be corrected through trial-and-error motor adaptation (e.g., (Kaernbach et al. 2002; Martin et al. 1996). In addition, the brain may recalibrate the relationship between the seen and felt position of the hand ($\Delta\hat{Y}_V$, $\Delta\hat{Y}_P$; e.g., (Harris 1963). The specific parameters of the task (visibility of the hand, presence of error feedback, etc) determine the extent to which perceptual vs. motor recalibration occurs (Welch 1986).

The visuomotor rotation or translation paradigm is a more recent, and more readily controlled, approach to studying the motor vs. sensory processes that occur in response to a visuo-proprioceptive mismatch. It entails deviating a cursor representing hand position by some offset. With practice and error feedback, participants adapt their movements so the cursor reaches the target. While visual realignment during motor adaptation has not been investigated to our knowledge, proprioceptive realignment has been found to occur during visuomotor rotation (Clayton et al. 2014; Cressman and Henriques 2009). Proprioceptive realignment arises with a different time course than motor adaptation (Ruttle et al. 2016;

Zbib et al. 2016) and does not generalize to perception of the body midline (Clayton et al. 2014), suggesting these are distinct processes. In fact, proprioceptive realignment itself may arise by two distinct mechanisms in a visuomotor adaptation task (Rossi et al. 2021). One mechanism requires systematic sensory prediction errors in proprioceptive feedback, which can occur with or without a visuo-proprioceptive mismatch (Rossi et al. 2021); this may explain the proprioceptive realignment observed in force field motor adaptation, which has no visuo-proprioceptive mismatch (Ostry and Gribble 2016). The other mechanism, which is the focus of the present study, is generally accompanied by visual realignment and specifically results from exposure to a visuo-proprioceptive mismatch (Rossi et al. 2021). Indeed, in a cursor rotation task, proprioceptive realignment occurs even without active movement (Mostafa et al. 2019) or movement error signals (Ruttle et al. 2018; Salomonczyk et al. 2013), consistent with the idea that a visuo-proprioceptive mismatch alone is sufficient to drive proprioceptive realignment.

The neural basis of motor adaptation has been explored in some depth, with many studies implicating the cerebellum and primary motor cortex (M1) (Caligiore et al. 2019). The trial-and-error process of adjusting motor commands to compensate for a systematic perturbation is known to depend on the cerebellum (Baizer et al. 1999; Bastian 2006; Block and Celnik 2013; Schlerf et al. 2012), and M1 is thought to play a role in storing and retaining these updates (Galea et al. 2011; Landi et al. 2011). The neural basis of visuo-proprioceptive realignment, on the other hand, is poorly understood. The form of proprioceptive realignment that results specifically from a visuo-proprioceptive mismatch appears unimpaired in individuals with cerebellar ataxia (Block and Bastian 2012). Because visuo-proprioceptive realignment involves multisensory processing, it is thought that multisensory regions of posterior parietal cortex could be involved (Andersen et al. 1997; Hagura et al. 2007, 2009). For example, the angular gyrus may mediate the normal relationship between visuo-proprioceptive weighting and visuo-proprioceptive realignment (Block et al. 2013).

Perhaps surprisingly given its traditional classification as a straightforward motor execution area (Hatsopoulos and Suminski 2011), M1 is also a potential substrate of visuo-proprioceptive realignment in response to a visuo-proprioceptive mismatch. M1 is closely interconnected with somatosensory cortex

(SI), and somatosensory responses have been recorded in M1 neurons (Hatsopoulos and Suminski 2011). M1 responds to kinesthetic illusions, and increases in excitability are attenuated by visual information that contradicts the illusion of movement, suggesting M1 involvement in relatively high level limb perception (Naito 2004). In addition, mirror activity has been found in M1 neurons, suggesting a capacity for visually-driven responses (Hatsopoulos and Suminski 2011). We recently assessed M1 excitability for an index finger representation with transcranial magnetic stimulation (TMS), before and after participants experienced misaligned or veridical visuo-proprioceptive information about that finger (Munoz-Rubke et al. 2017). The results suggest M1 activity is indeed associated with visuo-proprioceptive realignment in response to a visuo-proprioceptive mismatch. Changes were modality-specific, with a decrease in M1 excitability associated with proprioceptive realignment, and an increase in M1 excitability associated with visual realignment (Munoz-Rubke et al. 2017).

An important question that remains to be answered about M1 involvement in visuo-proprioceptive realignment concerns somatotopic specificity. If misaligned visuo-proprioceptive information about the index finger is presented, would changes to M1 and to body perception be limited to the representation of an index finger muscle (somatotopically focal: Fig. 1B), or would representations of the entire effector (including biceps and forearm muscles) be affected (somatotopically broad: Fig. 1C)? A somatotopically focal interaction would be consistent with the effects of peripheral somatosensory stimulation on M1. For example, vibration of one muscle increases M1 excitability for that muscle, but decreases it for neighboring muscles (Rosenkranz and Rothwell 2004). Neuroimaging suggests that M1 responses to illusory limb movement are somatotopically focal, in the sense that if the illusion involves wrist movement, only the wrist area of M1 responds (Naito 2004). However, a somatotopically broad interaction would make sense given that other limb segments are needed to move the realigned finger. This would be consistent with what we know of the generalization of motor learning within a limb. For example, when individuals learned a force production motor skill with their hand, it transferred to their arm and vice versa (Rajan et al. 2019).

Here we examined effects of a somatotopically localized visuo-proprioceptive perturbation on

M1 neurophysiology and conscious perception. In both domains, we asked whether such effects are specific to the brain's representation of the misaligned finger (somatotopically focal), or whether they extend to other parts of the hand and arm that would be needed to move the misaligned finger (somatotopically broad). In Experiments 1 and 2, we used TMS to measure M1 excitability for five hand and arm muscles, before and after participants experienced misaligned or veridical visuo-proprioceptive information about the index fingertip. In Experiment 3, we asked participants to indicate their proprioceptive estimate of four hand and arm joints, before and after misalignment at the fingertip, to assess the somatotopic focality of changes in perception.

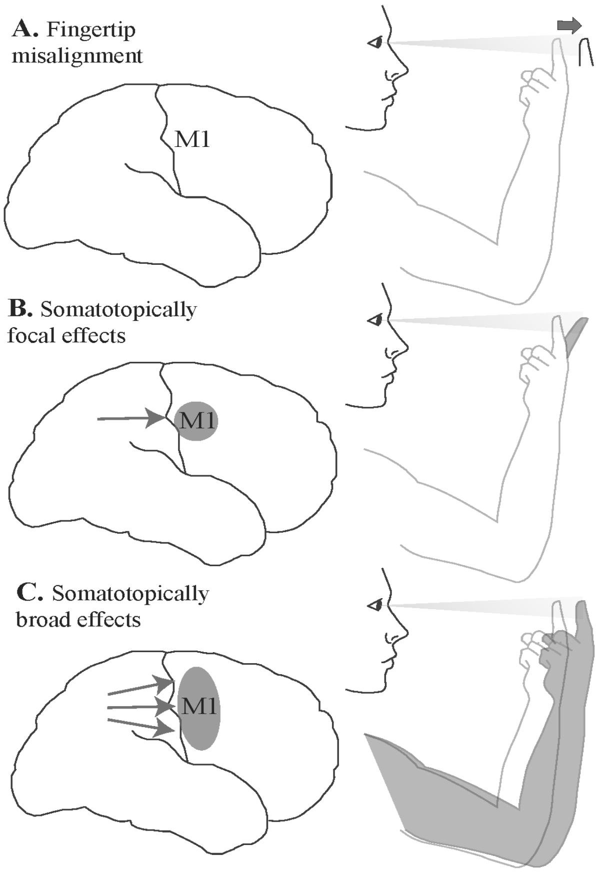

Figure 1. Visuo-proprioceptive representation of the body parts is both critical for motor control and highly plastic. **A.** Shifting visual information about the finger (solid finger) away from proprioceptive information (transparent finger) creates a visuo-proprioceptive mismatch. The brain compensates by realigning visual and proprioceptive estimates of finger position. This changes perceived finger position, which presumably affects motor planning, and has been linked to excitability changes in the M1 representation of that finger (Munoz-Rubke et al. 2017). However, the somatotopic specificity is unknown. **B.** One possibility is that such changes are somatotopically focal, affecting primarily the misaligned body part (grey finger) and thus distorting the body schema nearby. Neural changes associated with realignment, for example in the parietal lobe, are expected to affect only the finger area of M1 in this case (arrow). **C.** An alternative possibility is that the brain generalizes such changes more broadly, perhaps including other M1 representations needed to move the misaligned finger. In this case, neural changes in other brain regions would be expected to affect a broader area of M1 (arrows).

Methods

Participants

Participants in all three experiments were healthy right-handed young adults, with similar age ranges and gender balances. 27 individuals (21.7 ± 3.3 years, mean ± SD, 16 males) participated in Experiment 1. 26 individuals (21.9 ± 4.7 years, 9 males) participated in Experiment 2. Fourteen individuals participated in Experiment 3 (21.8 ± 2.49 years, 8 males). All participants reported themselves to be neurologically healthy with normal or corrected to normal vision. Experiment 1 and 2 participants additionally reported they were free from central nervous system-active drugs and other standard exclusion criteria for TMS studies (Rossi et al. 2009). All participants gave written informed consent. All procedures were approved by the Indiana University institutional review board.

Experiments 1 and 2: M1 hand and arm representation

Sessions. Participants completed two sessions each: the misaligned session (experimental) and the veridical session (control). In the misaligned session, a 70 mm misalignment between visual and proprioceptive information about the left index fingertip was gradually imposed. In the veridical session, visuo-proprioceptive information about the left index fingertip remained veridical throughout. The two sessions were separated by at least 5 days (mean 14.2 days, range 5-69 days) and session order was counterbalanced across participants.

In each session, TMS measurements were made pre- and post-perceptual alignment task (Fig. 2Ai). Experiments 1 and 2 were identical except for which M1 representations were targeted for TMS, and which muscles were recorded. In Experiment 1 (N = 27), TMS-evoked activity was recorded from two muscles in the left hand: first dorsal interosseus (FDI) and adductor digiti minimi (ADM). In Experiment 2 (N = 26), TMS-evoked activity was recorded from three muscles in the left arm: flexor carpi radialis (FCR), extensor carpi radialis (ECR), and biceps brachii (BB). At the end of each session in both experiments, participants were asked to rate their level of attention, fatigue, pain from TMS, and quality of sleep the night before, on a scale of 1-10, with 10 being the most attention, fatigue, or pain, and the best sleep. The purpose was to check for any major differences in participant state between sessions.

Perceptual alignment task setup and instructions. Participants were seated at a custom 2-D virtual reality apparatus (Fig. 2Aii) without vision of their arms. The apparatus contained a two-sided touchscreen consisting of two infrared touch overlays (PQLabs) with a 3-mm-thick pane of glass sandwiched between. This was positioned in the horizontal plane beneath the mirror, where participants viewed visual information that appeared to be in the plane of the touchscreen.

We used a bimanual task in which participants indicated with their right index fingertip (indicator finger) the position of three types of targets (Fig. 2Aiv) associated with the left index fingertip (target finger). The indicator finger remained above, and the target finger below, the touchscreen surface throughout the session. Visuo-proprioceptive (VP) targets consisted of the target fingertip, touching a tactile marker on the lower surface of the touchscreen, with a 1-cm white square projected on top. Visual-only (V) targets were indicated by the white square alone, with the target hand resting in the participant's lap. Proprioceptive-only (P) targets consisted of the target index finger placed on a tactile marker on the lower surface of the touchscreen, with no white square. *VP trials were used to create the misalignment while V and P trials were used to assess visual and proprioceptive realignment*. For P and VP trials, participants actively placed their target finger on the tactile marker. This active component is likely to increase the ratio of proprioceptive to visual realignment (Welch et al. 1979; Welch and Warren 1980) and encourage visuo-proprioceptive integration (Balslev et al. 2006).

Participants were told that on VP trials, the white box would appear directly over their target fingertip and that they should aim to place their indicator finger at that location. To best measure perceptual changes about the target finger and prevent motor adaptation of the indicator hand, (1) participants were instructed to reach at a comfortable pace, make adjustments if needed, and not to rush; (2) no online or endpoint feedback about the indicator hand was given at any point in the task; and (3) participants had no direct vision of either hand. As a result, participants did not know anything about their movement accuracy in indicating the positions of the targets, precluding motor adaptation of the indicator hand (for review see: (Shadmehr et al. 2010).

Perceptual alignment task procedures. At the start of every trial, an 8-mm blue cursor representing indicator finger position appeared to help participants place their indicator finger in the correct start position, which was represented as a yellow square. Once the indicator finger entered the yellow start square, the blue cursor disappeared so that no feedback was given regarding the movement of the indicator finger during the trial. As in previous studies, there were two possible target positions and five possible start locations, yielding 10 possible combinations that were presented in random order (Block et al. 2013; Liu et al. 2018; Munoz-Rubke et al. 2017). The five possible start positions were clustered at the participant's midline, about 15 cm in front of the participant's chest. The cluster was arranged like a plus sign, with each segment about 2 cm long. The two possible target positions were positioned 4 and 7 cm left of midline, about 33 and 36 cm in front of the participant's chest. The total display area was 75 × 100 cm. The use of multiple start and target positions was to add variability to the movement direction and extent of the indicator finger. One goal of adding this variability was to encourage participants to accurately indicate the perceived target position with their indicator finger, rather than make any stereotyped movements. A second goal was to make it less likely that participants would make systematically larger reaches in the misaligned session compared to the veridical session, due to the visuo-proprioceptive mismatch.

Throughout each trial, participants were told to focus their gaze on a red fixation cross. This was done to better capture changes in visual estimates of target position, as opposed to a change in eye position. While gaze direction could not be confirmed without gaze tracking technology, we encouraged participants to remember this instruction by playing a reminder at the start of every trial, before the "go" signal. The red cross appeared within a 10-cm zone around the target, with coordinates randomized across trials. Reaching performance has been shown to be somewhat affected by gaze direction (Henriques et al. 2003), but sometimes participants actually misunderstand the directions and attempt to place their indicator finger at the red cross, instead of at the target, especially on P targets where there is no other visual information. To evaluate whether this occurred, we computed a regression between red cross location and P target estimates (indicator finger endpoint position) for each session. For Experiment 1, this R^2 was 0.053 (mean) ± 0.011 (95% CI) in the misaligned session and 0.050 ± 0.014 in the veridical session. For Experiment 2, this R^2 was 0.050 ± 0.014 and 0.024 ± 0.006 in the misaligned and veridical sessions, respectively. These low values suggest that participants' target estimates were not likely influenced by the red cross position.

The perceptual alignment task portion of each session began with a 69-trial baseline of V, P, and VP trials, with the white square presented veridically over the target fingertip on VP trials (Fig. 2iv top row). The main portion consisted of 84 trials (42 VP, 21 V, and 21 P) presented in alternating order (VP, P, VP, V, etc). In the veridical session, target presentation was also veridical. However, in this portion of the misaligned session, the position of the white square was gradually shifted forward from the target finger in the positive y direction (away from the participant's body), 1.67 mm per VP trial (Fig. 2iv bottom row). On V trials, the white square was presented with the forward offset of the most recent VP trial. Thus, after 84 trials, there was a total misalignment of 70 mm between visual and proprioceptive information about the target fingertip. Most participants did not notice this gradual perturbation. At the end of each session, participants were asked "Did it feel like the white box was always on top of your target finger?" If they responded that it did not, we asked "In a particular direction, or all over the place?" If they indicated a particular direction, we asked them to estimate the magnitude. In Experiment 1, three participants reported a perceived forward displacement in the misaligned session only, one in the veridical session only, and one in both sessions. In Experiment 2, four participants reported a perceived forward displacement in the misaligned session only, and three reported this in the veridical session only. For participants who reported a forward offset, the median estimated magnitude of offset was 2.5 cm for Experiment 1 and 3 cm for Experiment 2. This is consistent with our previous use of this paradigm (Block et al. 2013; Munoz-Rubke et al. 2017); excluding these participants did not meaningfully change the multilevel modeling results, so they were left in.

Perceptual alignment task analysis. Spatial realignment of visual and proprioceptive estimates of target finger position were taken from V and P trials, respectively. If the proprioceptive estimate of the target finger, as shown by indicator finger endpoints, moves forward to reduce the visuo-proprioceptive gap ($\Delta\hat{y}_P$), then we observe overshoot on P targets. Similarly, if perceived position of the white square moves closer to the target finger ($\Delta\hat{y}_V$), then we observe undershoot on V targets. As we have done previously (Block et al. 2013; Block and Bastian 2011, 2012), we quantified visual and proprioceptive realignment ($\Delta\hat{y}_V$ and $\Delta\hat{y}_P$) in the misaligned session by subtracting indicator finger endpoint positions on the first four V or P trials of the misalignment phase from the last four:

$$\Delta\hat{y}_P = last\ 4\ P\ endpoints - first\ 4\ P\ endpoints \tag{1}$$

$$\Delta\hat{y}_V = 70 - (last\ 4\ V\ endpoints - first\ 4\ V\ endpoints) \tag{2}$$

Realignment was computed relative to actual target position, which does not change for P targets but shifts forward 70 mm for V targets during the misaligned session. Thus, for both modalities, realignment in the expected direction (i.e., overshoot for P targets and undershoot for V targets) comes out positive. These values were computed for the veridical session as well, using the first and last 4 V and P trials of the main 84 trials just like the misaligned session. $\Delta\hat{y}_V$ in the veridical session did not include subtraction from 70, since there was no 70 mm forward offset of the V target.

TMS setup and procedures. Before and after the perceptual alignment task in each session, TMS was used to measure the right hemisphere motor cortex excitability (Fig. 2Aiii); i.e., the hemisphere controlling the left (target) hand that experiences visuo-proprioceptive misalignment in the misaligned session but performs no motor task other than touching the tactile marker. During TMS, both arms rested on a pillow in the participant's lap. TMS was delivered using a Magstim 200^2 stimulator (Magstim Company LTD, UK) with a 70 mm figure-of-eight coil. The coil was positioned tangential to the skull with the handle pointing posteriorly, 45° to the inter-hemispheric line to evoke posterior-to-anterior current in the cortex (Rossini et al., 2015). We used a Brainsight neuronavigation system (Rogue Research) to record the hotspot for FDI (Experiment 1) or FCR (Experiment 2) at the beginning of each session to ensure consistent coil placement before and after the perceptual alignment task. Muscle activity was recorded with surface electromyography (EMG) using a belly-tendon montage, with a single common ground electrode over the ulnar styloid process (Experiment 1) or elbow (Experiment 2) of the target arm. We recorded from FDI and ADM in Experiment 1, and FCR, ECR, and BB in Experiment 2. EMG recordings were amplified (AMT-8; Bortec Biomedical), band-pass filtered (10-1000 Hz), sampled at

5000 Hz, and recorded on a hard drive for subsequent analysis using Signal software (Cambridge Electronic Design Ltd, UK) and MATLAB (Mathworks). Resting motor threshold (RMT) was measured at the beginning of each session. We determined RMT for either the FDI (Experiment 1) or FCR (Experiment 2) as the minimum stimulator intensity to evoke MEPs > 50 µV in at least 10 out of 20 trials (Rossini et al. 2015).

The input-output (I/O) curve was assessed immediately before and immediately after the perceptual alignment task in each session to quantify changes in excitability of the M1 representations of interest (Fig. 2Ai). To assess the I/O curve, monophasic single pulses were delivered at intensities ranging from 90% of RMT up to 200% of RMT, or as high as the participant could tolerate. The same TMS intensities were used before and after the misalignment task. Intensity order was randomized across participants and sessions but kept constant within a single session. The inter-pulse interval was 4-6 s. In Experiment 1, we delivered 10 pulses per intensity. In Experiment 2, we delivered 15 pulses per intensity since more proximal MEPs are more variable (Carson et al. 2013; Sankarasubramanian et al. 2015). The I/O curve procedure took about 15 minutes to complete. We expected that any changes in M1 excitability would last at least this long based on our previous study (Munoz-Rubke et al. 2017), as well as evidence that proprioceptive realignment associated with visuomotor adaptation is retained at least 24 hours (Nourouzpour et al. 2015).

Single trials in which root mean square EMG exceeded 15 microvolts in the 100 ms prior to the TMS pulse were excluded. For each I/O curve (2 per session per muscle per participant), MEP amplitude at each stimulus intensity was calculated and ordered by increasing stimulus intensity. Because not all participants could tolerate TMS intensities over 160% of RMT, and to be consistent with our previous use of this paradigm (Munoz-Rubke et al. 2017), we computed area under the I/O curve over the 90-160% of RMT range for all muscles except BB. This is common practice in both hand and forearm muscles (Carson et al. 2013; Rossini et al. 2015; Suzuki et al. 2014). However, because BB responses tend to be small when the FCR hotspot is targeted (Carson et al. 2013), for BB we computed area under the I/O curve from 90% of FCR RMT up to the participant's maximum tolerated intensity. This approach should partially compensate for not targeting the BB hotspot directly. Area under the I/O curve was calculated using the trapezoidal rule. We chose to focus on area under the I/O curve rather than slope, which is also commonly used, because I/O curves may take different shapes for different muscles, especially when slightly different stimulus intensities are captured for each muscle (Carson et al. 2013). In other words, a stimulus intensity of 120% of FCR RMT will yield a different place on the FCR I/O curve than on the BB I/O curve, since the BB hotspot is somewhat different from the FCR hotspot (Carson et al. 2013). Importantly, I/O curves were only compared to other I/O curves obtained from the same muscle.

Statistical analysis. To test whether changes in excitability of any of the muscles was related to individual responses to misalignment, we computed a multilevel linear model for percent change (post-alignment task divided by pre) in area under the I/O curve in association with session type (misaligned or veridical). A separate multilevel model was computed for each muscle (FDI and ADM in Experiment 1; FCR, ECR, BB in Experiment 2). Consistent with our previous study (Munoz-Rubke et al. 2017), we computed a reduced model that included only the interaction terms; in other words, the minimum predictors needed to reveal whether individuals' visual and proprioceptive realignment was related to their change in M1 excitability. The fixed part of each model thus comprised interaction terms of session type with proprioceptive realignment and visual realignment. The models also included a random intercept to account for the repeated-measures design. All models were computed with the lmer4 package, Version 1.1.12 (Bates et al. 2015), and displayed using the sjPlot package, Version 2.8.7 (Daniel Lüdecke 2021), of the R programming language (R Core Team 2016). Predictor significance was estimated using the test statistic (t) calculated from the parameter estimate divided by SE. P-values were calculated based on the t-statistic with corresponding degrees of freedom. Pearson correlations between realignment residuals and log-transformed percentage of baseline area under the I/O curve were computed to provide an effect size (r) for each parameter estimate.

We checked whether the I/O curves were normally distributed using the Shapiro-Wilk test. This indicated that area under the I/O curve was not normally distributed for any muscle in any session, and percent change in area under the I/O curve was non-normal for certain muscles in certain sessions: FDI

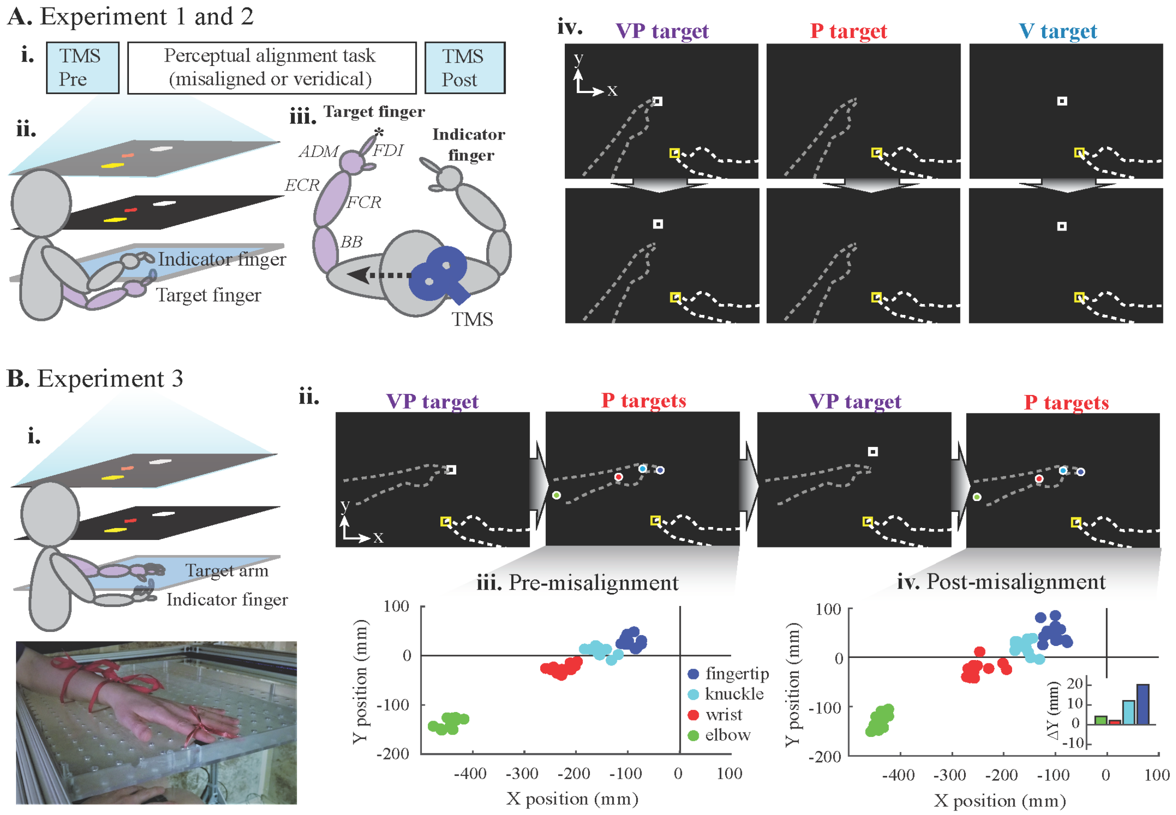

Figure 2. Methods. **A.** Expt. 1 and 2. **i.** Session design. Each participant completed two sessions, distinguished by the VP target being veridical throughout (control) or gradually misaligned. **ii.** Perceptual alignment task apparatus. Images viewed in the mirror (middle layer) appeared to be in the plane of the touchscreen glass (bottom layer). Participants pointed with their right (indicator) index finger above the glass to where they perceived targets related to their left (target) index finger, which was positioned on a tactile marker beneath the glass (purple). **iii.** TMS over right M1 was used to assess I/O curves in the left, target limb (purple). *Site of misalignment. **iv.** Indicator finger began in yellow start box and moved to perceived location of a white box (V target), left fingertip (P target), or both together (VP target). Dashed lines not visible to participant. No performance feedback. Bottom row: In misaligned session only, white box gradually shifted forward. **B.** Expt. 3. **i.** Participants pointed with their right (indicator) index finger beneath the glass to where they perceived targets related to their left hand or arm, which rested on top of the glass. **ii.** Two blocks of P trials alternated with two blocks of VP trials. For P target blocks, participants pointed to their unseen left index fingertip (blue), knuckle (cyan), wrist (red) or elbow (green). In VP target blocks, left index fingertip position was indicated by a white square that gradually shifted forward in the second (misaligned) VP block. Lower panels: A single participant's performance on P targets before and after the VP misalignment block. Left index fingertip was always at the origin. Joint estimates shifted forward relative to pre-misalignment (inset), suggesting proprioceptive realignment in response to the VP misalignment block.

misaligned and ADM veridical session in Experiment 1, and FCR veridical and BB misaligned session in Experiment 2 (all $p < 0.05$). We therefore log-transformed these variables for all five muscles, in both sessions. This resulted in all variable distributions meeting the assumption of normality. For each muscle, no predictor had a variance inflation factor value greater than 1.5, suggesting the absence of multicollinearity in the multilevel models. We checked for potential outliers by calculating Cook's distance (Nieuwenhuis et al. 2012). No data point showed a D value > 1, suggesting no outliers were present for any of the muscles (Cook and Weisberg 1982). To examine the raw I/O curves we computed a repeated measures ANOVA with factors Session (misaligned vs. veridical) and Timepoint (pre- vs. post-alignment task) on the log-transformed area under the I/O curve. We computed partial eta squared (η_p^2) as an effect size for all ANOVA effects. All hypothesis tests were performed with $\alpha = 0.05$.

Experiment 3: Hand and arm proprioception

Each participant completed one session. The session consisted of a modified version of the perceptual alignment task used in Experiments 1 and 2. Participants were asked to indicate with their right index finger the position of a target related to the left hand or arm.

Apparatus and setup. The same apparatus was used as in the first two experiments, with no direct vision of either hand or arm. The indicator finger was again the right index finger, but proprioceptive targets included four points on the left hand and arm: index fingertip, knuckle (anterior first metacarpophalangeal (MP) joint), wrist (anterior midline), and elbow (medial epicondyle). A small square of tape (~5 mm) was placed on each joint to make sure the participant understood which part of each joint to aim for. Participants were instructed to aim for the center of the tape. To avoid fatiguing the target arm, the participant's left hand and forearm were rested on top of the touchscreen glass, palm down, fingers spread, and slightly to the right of body midline (Fig. 2Bi).

Prior to the participant placing their left arm in this position, a thin plastic pegboard was secured onto the touchscreen glass. The index fingertip was first placed on a tactile marker on the pegboard, to ensure the fingertip would be at the same location as the visual target projection. The wrist and elbow were then placed on the pegboard in a way that allowed the fingertip to remain on the tactile marker. Once the participant was comfortable, the left arm was tied to the pegboard at the index finger, the wrist, and the forearm. When positioned, the elbow was bent at about 90 degrees and the wrist was straight. Participants were asked to keep their target arm and hand relaxed and still except during breaks.

The right indicator hand remained below the glass at all times, indicating position estimates on the lower surface of the glass.

Procedures. The session consisted of alternating blocks of two types: proprioceptive-only (P targets) and visuo-proprioceptive (VP targets). For each P target block, participants were asked to indicate their estimate of the left index fingertip, knuckle, wrist, and elbow, 12 times each in random order (48 trials total in the block). No visual information was given about any of the proprioceptive targets during the P block. Each VP block consisted of 42 VP trials in which the participant was asked to indicate their estimate of the left index fingertip with a white box they were told was at the same location.

The session began with a familiarization of the P targets. This was followed by a veridical VP block, a pre-misalignment P block, then a VP block in which misalignment occurred, and finally a post-misalignment P block (Fig. 2Bii). During the misalignment VP block, the white box was gradually shifted forward (positive y-dimension) from the left index fingertip, 1.67 mm every other trial, for a maximum misalignment of 35 mm. To maintain circulation and comfort, participants were given a short break between blocks to isometrically contract their left arm, which remained in the same position on the pegboard throughout. They were instructed to do shoulder rolls and to press down with their fingers, hand, and forearm, and then relax. At the conclusion of the experiment, participants were asked to rate their fatigue, attention, and sleep quality from the previous night on a scale from 1-10.

Each trial began with the right (indicator) hand resting in the participant's lap. The target arm remained positioned on the pegboard throughout. As in Experiments 1 and 2, participants were instructed to fixate on the red fixation cross, which appeared at random coordinates within a 10 cm zone around the fingertip target. After an auditory signal, participants indicated their perception by moving their right index fingertip to the lower surface of the glass under which they felt the target was located. As in Experiments 1 and 2, participants had no direct vision of their arms; received no performance feedback or knowledge of results; had no speed requirements; and were asked to be as accurate as possible. During P target blocks, the specific joint to aim for on each trial was indicated to the participant by text along the top of the reflected display: finger, knuckle, wrist, or elbow.

As with Experiments 1 and 2, we calculated a regression between red cross position and indicator finger endpoints on P fingertip targets. The group average R^2 was 0.032 ± .019 (mean ± 95% CI), which is consistent with Experiments 1 and 2. We also questioned participants about whether the white box felt like it was on top of their target fingertip. None reported perceiving a forward offset of the white box.

Analysis. For each participant, we calculated the change in each joint's proprioceptive estimate from pre-misalignment to post-misalignment, in the dimension of misalignment (y-dimension; see Fig. 2Bii bottom panels). To compare realignment at the knuckle, wrist, and elbow to realignment at the fingertip, we computed a correlation between realignment at the fingertip and at each of the other joints. Realignment at all four joints appeared normally distributed (Shapiro-Wilk $p > 0.56$). Pearson correlation coefficients were calculated with an α of 0.05, and results are reported after Bonferroni correction.

Results

Experiment 1: M1 hand representations

Behavioral results. On average, participants had 15.2 ± 5.2 days between the two sessions (mean ± 95% CI). On a scale of 1-10, participants rated their quality of sleep the night before at 7.7 ± 0.6 for the misaligned session and 7.6 ± 0.4 for the veridical session. They rated their level of attention at 7.5 ± 0.4 and 7.9 ± 0.4 for the misaligned and veridical sessions, respectively. They rated their fatigue from the experiment at 4.3 ± 0.7 and 3.7 ± 0.8 for the misaligned and veridical sessions, respectively.

Because no misalignment occurred in the veridical session, visual and proprioceptive realignment are expected to be roughly zero on average, across participants, whereas in the misaligned session we expect them to be above zero on average. In the misaligned session, participants realigned proprioception 14.5 ± 4.2 mm (mean ± 95% CI), range, and vision 33.9 ± 6.4 mm (Fig. 3Ai and Bi). Including both visual and proprioceptive realignment, participants compensated for 48.4 ± 6.1 mm of the 70 mm visuo-proprioceptive mismatch. Any combination of visual and proprioceptive realignment can be used to compensate for the misalignment in this task. Visual and proprioceptive were inversely correlated in the misaligned session (Fig. 4), meaning that participants who realign vision a large amount tend to realign proprioception a small amount, and vice versa.

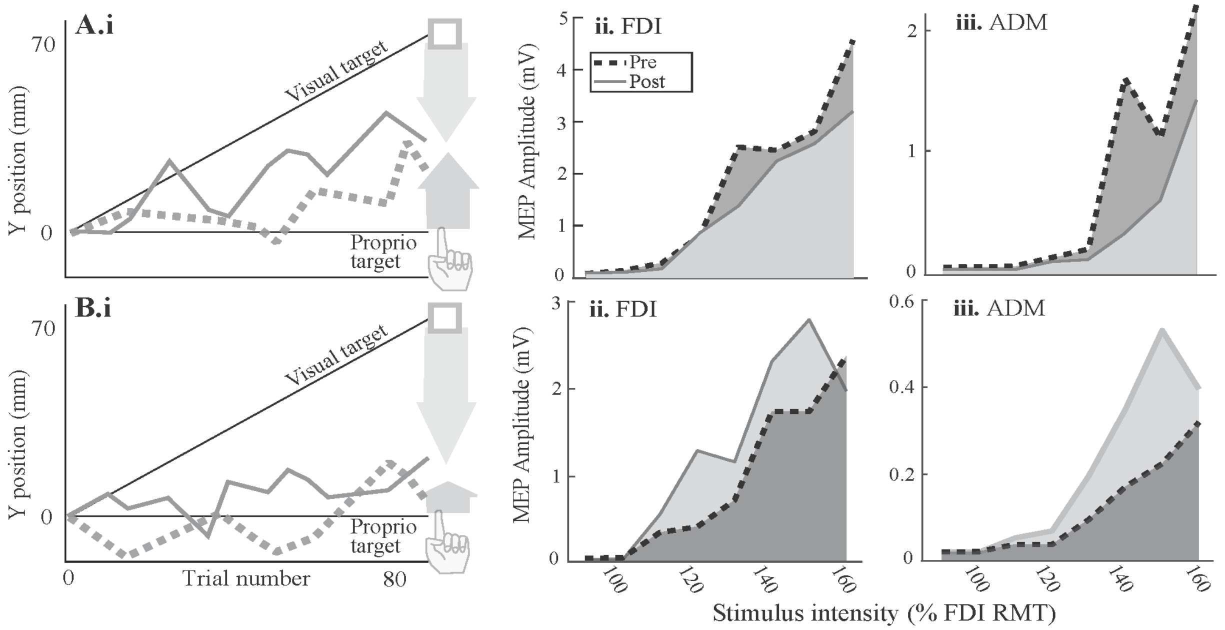

Figure 3. Comparison of two participants from Expt. 1. **A.i.** This individual realigned proprioception 37.1 mm (dashed grey line, bottom arrow) and vision 29.8 mm (solid thick grey line, top arrow). **ii-iii.** Area under the I/O curve decreased after the misaligned task 23% for FDI and 52% for ADM. **B.i.** In the misaligned session, this participant realigned proprioception 12.3 mm (bottom arrow) and vision 57.5 mm (top arrow). **ii-iii.** Area under the I/O curve increased after misaligned task 52% for FDI and 90% for ADM.

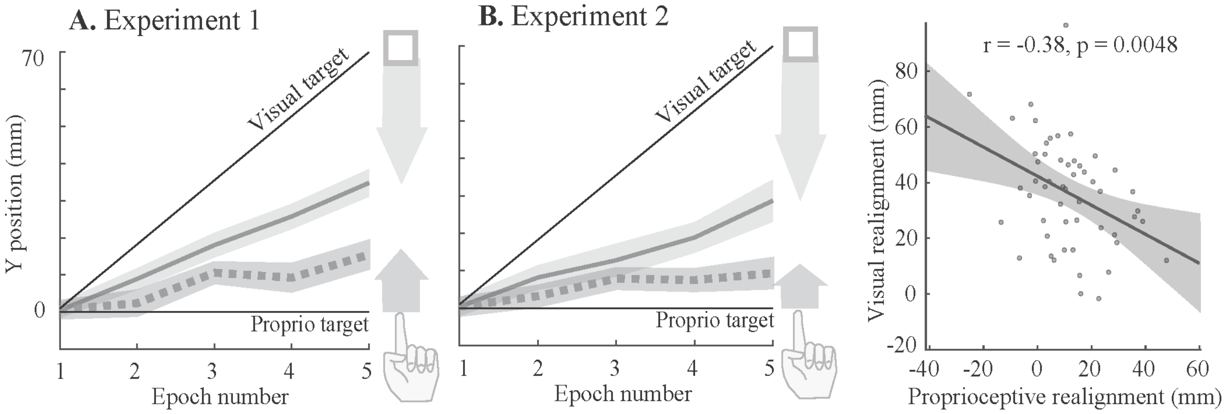

Figure 4. Group behavioral results from Expt. 1 and 2. **A-B.** Experiment 1 and 2 misaligned sessions. Mean visual (thick line) and proprioceptive (dashed line) position estimates, in epochs of 4 trials. Changes in both modalities appear roughly linear. Visual realignment (light grey arrow) was greater than proprioceptive (dark grey arrow) for both experiments. **C.** Visual vs. proprioceptive realignment magnitudes, participants pooled across Expt. 1 and 2 misaligned session. Negative correlation indicates that participants who realign vision a large amount tend to realign proprioception a small amount, and vice versa.

In the veridical session, participants realigned proprioception 0 ± 4.9 mm and vision -3.3 ± 5.0 mm. These values are consistent with our previous use of this paradigm (Munoz-Rubke et al. 2017). We also compared variance of indicator finger positions on VP targets in the first vs. second half of the task, to evaluate whether pointing variance generally decreased across trials. The early-to-late change in variance did not differ significantly across sessions ($t_{26} = 1.40$, $p = 0.17$).

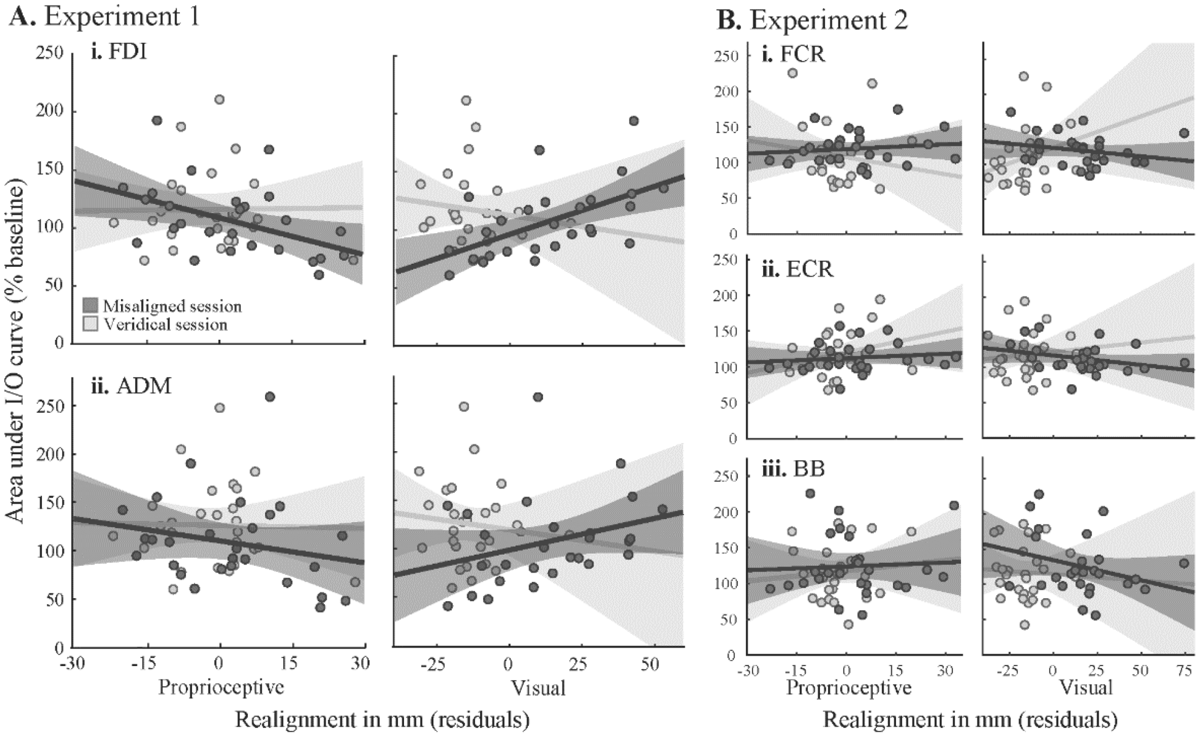

Figure 5. Change in area under the I/O curve (post divided by pre) plotted against predictor residuals, with lines of best fit and corresponding 95% CIs. Predictor residual plots allow us to show the relationship of one predictor variable (e.g., proprioceptive realignment) with the dependent variable, after statistically controlling for the effect of the other predictor (visual realignment), and vice versa. In the misaligned session, realignment of either modality in the positive direction is beneficial (i.e., helps compensate for the visuo-proprioceptive mismatch). **A. Experiment 1.** For both FDI (i) and ADM (ii), after statistically controlling for the effect of visual realignment, large proprioceptive realignment in the misaligned session (dark grey) was significantly associated with reduced M1 excitability (left panels). For FDI only, after controlling for the effect of proprioceptive realignment, large visual realignment was associated with increased M1 excitability (right panel). No associations found in veridical session (light grey). **B. Experiment 2.** No significant associations were found for FCR (i), ECR (ii), or BB (iii).

Neurophysiology. Changes in excitability of the M1 representation of FDI showed realignment modality-specific associations with the misaligned, but not the veridical session. These associations are illustrated with predictor residual plots (Fig. 5Ai), which allows us to show the relationship of one predictor variable with the dependent variable, after statistically controlling for the effect of the other predictor (McElreath 2015). In other words, for the misaligned session only, greater positive proprioceptive realignment (more overshoot of P targets) was associated with greater decrease in area under the I/O curve, after controlling for the effect of visual realignment. Conversely, after controlling for the effect of proprioceptive realignment, greater positive visual realignment (more undershoot of V targets) was associated with more increase in area under the I/O curve. For either modality, realignment in the positive direction is beneficial (i.e., helps compensate for the visuo-proprioceptive mismatch).

The multilevel model of the association between log percent change in area under the FDI I/O curve and session type (Table 1) indicates a negative association between the misaligned session and proprioceptive realignment ($\beta = -0.01$, $t_{47} = -2.85$, $p = 0.004$) and a positive association between the misaligned session and visual realignment ($\beta = 0.004$, $t_{47} = 1.99$, $p = 0.047$). These may be considered a medium ($r = -0.49$) and large ($r = 0.60$) effect size, respectively (Cohen 1992). With the dependent variable log-transformed, the betas can be interpreted by exponentiating. The negative association between misaligned session and proprioceptive realignment is equivalent in magnitude to a 1.01% more reduction in FDI area under the I/O curve for every 1 mm more of positive proprioceptive realignment. The positive association between misaligned session and visual realignment can be interpreted as a 0.37% more increase in FDI excitability for every 1 mm more of positive visual realignment.

Full model results are presented in Supplementary Table S1. No statistically significant associations were observed during the veridical session ($p > 0.3$), and effect sizes would be considered small (Table S1). From the perspective of a single participant in the misaligned session, individuals who realigned proprioception by a relatively large magnitude in the positive (beneficial) direction generally had a *decrease* in excitability for the M1 representation of FDI. The first example participant (Fig. 3A) is consistent with this pattern; she had a relatively large proprioceptive realignment magnitude and I/O curves showing a decrease in M1 excitability. Individuals who realigned vision by a relatively large magnitude in the positive direction generally had an *increase* in M1 excitability of the FDI representation. The second example participant (Fig. 3B) is consistent with this pattern; he had a relatively large amount of visual realignment and small amount of proprioceptive realignment, and his I/O curves showed an increase in excitability.

The multilevel model for ADM also showed a significant association for the misaligned session (Fig. 5Aii). Specifically, a negative association between the misaligned session and proprioceptive realignment was observed ($\beta = -0.01$, $t_{47} = -2.43$, $p = 0.015$; Table 1). This is equivalent to a 1.27% decrease in ADM area under the I/O curve for every 1 mm more of proprioceptive realignment, and can be considered a medium effect size ($r = -0.34$). The association between the misaligned session and visual realignment was positive, but not statistically significant ($\beta = 0.002$, $t_{47} = 0.81$, $p = 0.42$), although the effect size ($r = 0.41$) can be considered medium (Cohen 1992). Full model results are presented in Supplementary Table S2. No statistically significant associations were observed during the veridical session ($p > 0.5$), and effect sizes would be considered small (Table S2). At the individual participant level, participants who realigned proprioception substantially in the misaligned session tended to have a greater reduction in M1 excitability of the ADM representation.

Table 1. Experiment 1 multilevel regression results comprising four interaction terms for session type (veridical or misaligned) and realignment type (proprioceptive or visual)

	FDI		ADM	
Predictors	*β (CI)*	*p*	*β (CI)*	*p*
Fixed parts				
Intercept	4.69 (4.60, 4.79)	**<0.001**	4.74 (4.60, 4.89)	**<0.001**
Veridical session : Proprioceptive realignment	0.0016 (-0.0075, 0.0108)	0.723	-0.0005 (-0.014, 0.013)	0.939
Misaligned session : Proprioceptive realignment	-0.010 (-0.017, -0.003)	**0.004**	-0.013 (-0.023, -0.002)	**0.015**
Veridical session : Visual realignment	-0.0040 (-0.013, 0.0049)	0.375	-0.004 (-0.017, 0.009)	0.534
Misaligned session : Visual realignment	0.0037 (0.0000, 0.0073)	**0.047**	0.0022 (-0.0031, 0.0075)	0.418
Random parts				
N_{ID}	27		27	
Observations	54		54	

Columns represent log-transformed percentage of baseline (post divided by pre) in area under the I/O curve. βs are presented with their 95% CIs. Boldface identifies statistically significant results.

Other measures related to M1 neurophysiology and TMS were similar between the misaligned and veridical sessions. For FDI, ANOVA of log-transformed area under the I/O curve showed a main effect of timepoint ($F_{1,26} = 5.83$, $p = 0.023$, $\eta_p^2 = 0.18$), but no effect of session ($F_{1,26} = 1.38$, $p = 0.25$, $\eta_p^2 = 0.050$) and no timepoint X session interaction ($F_{1,26} = 1.47$, $p = 0.24$, $\eta_p^2 = 0.054$). This suggests an increase in excitability for the M1 representation of FDI related to the alignment task, regardless of whether it was the misaligned or veridical task (see Supplementary Fig. S1Ai). For ADM (Fig. S1Aii), log-transformed area under the I/O curve showed no significant effect of timepoint ($F_{1,26} = 2.95$, $p = 0.098$, $\eta_p^2 = 0.102$), session ($F_{1,26} = 0.008$, $p = 0.92$, $\eta_p^2 = 0.0003$), or interaction ($F_{1,26} = 3.13$, $p = 0.088$, $\eta_p^2 = 0.11$). On a scale from 1-10, participants rated the painfulness of TMS at 2.7 ± 0.7 and 2.7 ± 0.6 for the misaligned and veridical sessions, respectively (mean ± 95% CI). FDI RMT was 40.5 ± 2.3% of max stimulator output in the misaligned session, and 41.3 ± 2.3% of max stimulator output in the veridical session.

Experiment 2: M1 arm representation

Behavioral results. Participants had 13.3 ± 5.3 days between the two sessions (mean ± 95% CI). On a scale of 1-10, participants rated their quality of sleep the night before at 6.9 ± 0.5 for the misaligned session and 7.4 ± 0.6 for the veridical session. They rated their level of attention at 7.2 ± 0.6 and 7.4 ± 0.5 for the misaligned and veridical sessions, respectively. They rated their fatigue from the experiment at 4.3 ± 0.7 and 4.1 ± 0.8 for the misaligned and veridical sessions, respectively.

As in Experiment 1, realignment magnitudes in Experiment 2 were consistent with our previous use of this paradigm (Munoz-Rubke et al. 2017). In the misaligned session, participants realigned proprioception 9.0 ± 6.3 mm (mean ± 95% CI), and vision 38.2 ± 8.5 mm (Fig. 4B). Including both visual and proprioceptive realignment, participants compensated for 47.2 ± 8.5 mm of the 70 mm visuo-proprioceptive mismatch. In the veridical session, participants realigned proprioception 2.8 ± 3.9 mm and vision 5.1 ± 4.8 mm. We also compared variance of indicator finger positions on VP targets in the first vs. second half of the task, to evaluate whether pointing variance generally decreased across trials. The early-to-late change in variance did not differ significantly across sessions ($t_{25} = 0.31$, $p = 0.76$).

Neurophysiology. Multilevel model results do not indicate any realignment modality-specific associations with the misaligned session for FCR (Fig. 5Bi), ECR (Fig. 5Bii), or BB (Fig. 5Biii). All effect sizes would be considered small (Cohen 1992). In other words, neither visual nor proprioceptive realignment was significantly associated with log percent change in area under the I/O curve for any of the three muscles recorded in Experiment 2; this is seen even in participants who realigned the most. Multilevel model results are summarized in Table 2, and presented in full in Supplementary Table S3, Table S4, and Table S5. At baseline, visual and proprioceptive estimates were correlated across sessions ($r = 0.64$ and 0.68, $p < 0.001$), as was area under the I/O curve for FCR, ECR, and BB ($r = 0.71, 0.50, 0.52$; $p = 0.001, 0.014, 0.007$). These large effect sizes (Cohen 1992) are consistent with good between-session reliability of these measures.

Table 2. Experiment 2 multilevel regression model results comprising four interaction terms for session type (veridical or misaligned) and realignment type (proprioceptive or visual).

	FCR		ECR		BB	
Predictors	*β (CI)*	*p*	*β (CI)*	*p*	*β (CI)*	*p*
Fixed parts						
Intercept	4.66 (4.55, 4.77)	**<0.001**	4.71 (4.63, 4.80)	**<0.001**	4.75 (4.61, 4.89)	**<0.001**
Veridical session : Proprioceptive realignment	-0.0089 (-0.0202, 0.0024)	0.124	0.0073 (-0.0012, 0.0158)	0.093	0.0039 (-0.0112, 0.0190)	0.612
Misaligned session : Proprioceptive realignment	0.0022 (-0.0039, 0.0083)	0.483	0.0014 (-0.0034, 0.0061)	0.572	0.0023 (-0.0057, 0.0104)	0.57
Veridical session : Visual realignment	0.0092 (-0.0002, 0.0187)	0.055	0.0011 (-0.0062, 0.0083)	0.773	-0.0038 (-0.0162, 0.0087)	0.555
Misaligned session : Visual realignment	0.0016 (-0.0013, 0.0045)	0.285	-0.0006 (-0.0027, 0.0015)	0.577	-0.0007 (-0.0048, 0.0034)	0.737
Random parts						
N_{ID}	26		26		26	
Observations	52		52		52	

Columns represent log-transformed percentage of baseline (post divided by pre) in area under the I/O curve. βs are presented with their 95% CIs. Boldface identifies statistically significant results.

In contrast, all three muscles showed a significant increase in log area under the I/O curve from pre- to post-alignment task (ANOVA main effect of timepoint: $F_{1,25} = 5.82$, $p = 0.023$, $\eta_p^2 = 0.19$ for FCR; $F_{1,25} = 10.7$, $p = 0.003$, $\eta_p^2 = 0.30$ for ECR; and $F_{1,25} = 9.30$, $p = 0.005$, $\eta_p^2 = 0.27$ for BB), which can each be considered a large effect size (Cohen 1992). This suggests the M1 representation of all three muscles increased in excitability after the task, regardless of whether it was the misaligned or veridical session (Fig. S1B). FCR had no effect of session ($F_{1,25} = 0.02$, $p = 0.88$, $\eta_p^2 = 0.0009$) and a timepoint X session interaction that did not rise to the level of significance ($F_{1,25} = 3.53$, $p = 0.072$, $\eta_p^2 = 0.12$). ECR had no session effect ($F_{1,25} = 1.97$, $p = 0.17$, $\eta_p^2 = 0.073$) and no interaction ($F_{1,25} = 0.33$, $p = 0.57$, $\eta_p^2 = 0.013$).

BB had no significant effect of session ($F_{1,25} = 4.05$, $p = 0.055$, $\eta_p^2 = 0.14$) and no timepoint X session interaction ($F_{1,25} = 0.40$, $p = 0.53$, $\eta_p^2 = 0.016$). This suggests that BB excitability in the two sessions was slightly different, both before and after the alignment task, but did not change differently from pre- to post-alignment task in one session compared to the other.

On a scale from 1-10, participants rated the painfulness of TMS at 1.8 ± 0.3 and 2.0 ± 0.6 for the misaligned and veridical sessions, respectively (mean ± 95% CI). FCR RMT was 41.4 ± 2.4% of max stimulator output in the misaligned session, and 40.8 ± 2.1% of max stimulator output in the veridical session.

Experiment 3: Hand and arm proprioception

After a 35 mm visuo-proprioceptive misalignment at the left index fingertip, some participants showed a marked forward shift in in their proprioceptive estimate of that finger (e.g., Fig. 2Bii bottom). However, on average proprioceptive realignment was 1.9 ± 4.4 mm (mean ± 95% CI) at the fingertip. Knuckle, wrist, and elbow realignment averaged -0.4 ± 4.7 mm, -3.2 ± 3.2 mm, and 4.6 ± 4.2 mm, respectively. Fingertip realignment was most closely related to proprioceptive realignment at the knuckle (Fig. 6A), with a correlation of 0.78 ($p = 0.0033$), which can be considered a large effect size (Cohen 1992). However, proprioceptive realignment at the wrist was not significantly correlated

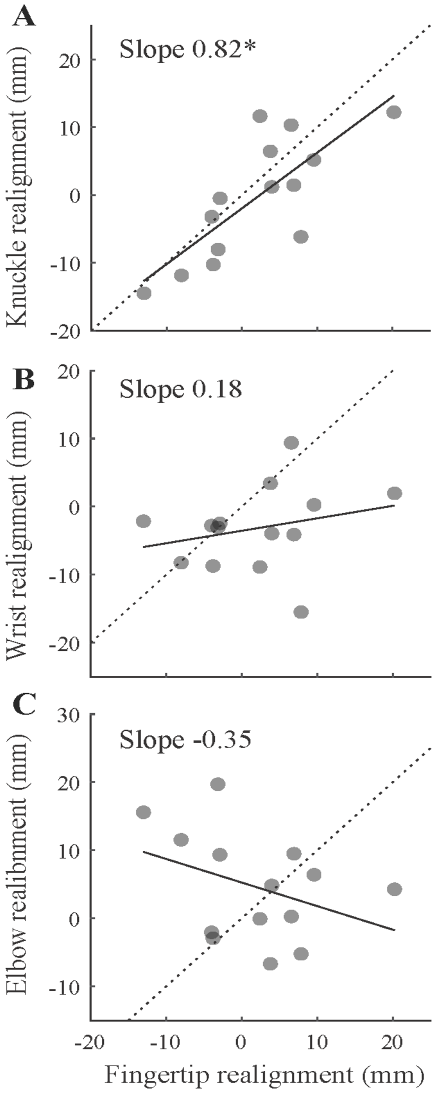

Figure 6. Experiment 3 results. Realignment in proprioceptive estimates of the knuckle (**A**), wrist (**B**), and elbow (**C**) targets, compared to proprioceptive realignment at the left index fingertip. Dotted line represents a 1:1 relationship between realignment at the two joints. Each circle represents one participant. *Correlation $p < 0.05$.

with realignment at the fingertip (r = 0.25, p > 0.9; Fig. 6B), and neither was proprioceptive realignment at the elbow (r = -0.37, p = 0.57; Fig. 6C). These correlations can be considered a small and medium effect size, respectively (Cohen 1992). On a scale of 1-10, the 14 participants rated their quality of sleep at 6.9 ± 0.7, their level of attention at 6.6 ± 1.1, and their level of fatigue at 4.4 ± 1.2.

Discussion

Here we asked whether visuo-proprioceptive realignment at the fingertip affects only the brain's representation of the misaligned finger (somatotopically focal), or whether changes extend to other parts of the hand and arm that would be needed to move the misaligned finger (somatotopically broad). Results from three experiments support the first option (Fig. 1B): at both the level of M1 neurophysiology and conscious perception, hand regions near the misaligned fingertip were affected, but further parts of the limb were not.

Visual and proprioceptive realignment of target fingertip position estimate

Consistent with our previous uses of the misalignment paradigm (Block et al. 2013; Block and Bastian 2011, 2012; Block and Sexton 2020; Munoz-Rubke et al. 2017), participants in Experiment 1 and 2 compensated for about two-thirds of the 70 mm visuo-proprioceptive mismatch, counting both visual and proprioceptive realignment. The magnitude of visual realignment was higher than the magnitude of proprioceptive realignment, which is also consistent with our previous work, and could be interpreted as an indication that proprioception is more reliable, and weighted higher, than vision (Ghahramani et al. 1997). Although vision has been said to dominate or "capture" proprioception (Botvinick and Cohen 1998; Hagura et al. 2007), the relative reliability of vision and proprioception is not constant and depends on environmental and computational factors. Thus, there are many circumstances where other modalities are relied on as much as or more than vision (van Beers et al. 2002; Ernst and Banks 2002; Mon-Williams et al. 1997; Naito 2004; Shams et al. 2000). Indeed, many of our participants have greater precision in their proprioceptive estimates than their visual estimates (Liu et al. 2018). The brain may take the cost of coordinate transformations into account, weighting proprioception higher for proprioceptive targets and vision higher for visual targets (Sober and Sabes 2005). Proprioception is more reliable than vision in the sagittal dimension (van Beers et al. 1996, 1999, 2002), which was the dimension of misalignment in the present study.

Another factor that likely increased visual relative to proprioceptive realignment was the random fixation point. Fixation was incorporated for two reasons: (1) To standardize behavior during proprioceptive targets by discouraging participants from gazing at where they think their finger is, thereby adding eye position signals; and (2) To dissociate eye position from location on the retina, so that visual realignment could reflect a change in visual spatial perception, not simply a change in the eye position-target mapping. Had participants been freely permitted to stare at the visual target, this would likely increase visual target salience and reduce associated noise, due to the additional spatial information from eye muscles. Both effects would result in up-weighting of vision (Block and Bastian 2010) and likely a smaller magnitude of visual realignment and larger magnitude of proprioceptive realignment (Block and Bastian 2011; Ghahramani et al. 1997).

One potential concern in a task with forward-displacement of the visual target is the meaning of target undershoot. We quantified visual realignment as undershooting of the forward-shifted visual target, but we cannot rule out the possibility that some portion of this undershoot was due to participant "laziness" or tendency to conserve effort. However, it should be noted that the main conclusions of the present study do not depend on a group average magnitude of visual realignment, which could be affected by a tendency to conserve effort.

M1 representation of the misaligned index finger showed realignment-specific changes

Results from FDI in Experiment 1 are consistent with our previous findings (Munoz-Rubke et al. 2017): Area under the I/O curve decreased in association with proprioceptive realignment, and increased in association with visual realignment in the misaligned session. In other words, M1 excitability changes were specific to the sensory modality of realignment. This is consistent with a neurological model in which changes in visuo-proprioceptive integration are reflected in M1 via altered connections from brain areas traditionally considered unisensory, such as SI (Krubitzer and Kaas 1990; Ostry and Gribble 2016) or early visual areas that have indirect connectivity with M1 (Strigaro et al. 2015). While multisensory influences on M1 have rarely been studied, proprioceptive training (Wong et al. 2012) and stimulation (Carel et al. 2000; Lewis and Byblow 2004) are known to affect movement and motor system plasticity, respectively

The modality-specific associations for FDI representation were present in the misaligned, but not the veridical (control) session, suggesting a specific connection to visuo-proprioceptive realignment. Furthermore, although raw visual and proprioceptive realignment were inversely correlated (participants who realign proprioception a great deal realign vision relatively little, and vice versa), this is controlled for by the multilevel model. In other words, the relationship between visual realignment and percent change in FDI area under the I/O curve depicted in the residual plots and model tables is a relationship that exists *after* statistically controlling for proprioceptive realignment.

In a bimanual task such as the misalignment task, it is important to establish that any processes other than visuo-proprioceptive realignment at the target finger were controlled for. A bimanual alignment task combines motor noise in the indicator hand with sensory noise in both hands. However, motor and sensory noise related to the indicator finger is consistent across all three trial types. Thus, any differences among indicated positions of V, P, and VP targets are attributable to differences in participants' perceptions of the target. Importantly, indicator finger movements are varied by the use of 5 start and 2 target positions, so data are unlikely to be influenced by motor memory.

We chose to assess M1 excitability changes in the non-dominant hand/cortex because the dominant limb is thought to be specialized for movement trajectory control while the nondominant limb is specialized for holding static postures (Sainburg 2002). For example, most people hammering a nail would hold the nail with the nondominant hand and swing the hammer with their dominant hand. In keeping with this natural behavior, we chose to use the nondominant limb as the static target and the dominant limb as the indicator. If this were reversed and we measured the dominant hemisphere, it is possible the neurophysiological effects could be stronger. However, the behavioral data might be messier due to greater motor noise associated with trajectory control with the nondominant limb used as the indicator. Understanding the lateralization of this phenomenon will require further studies.

Another potential concern is whether the indicator hand could undergo motor adaptation. Motor learning is possible in the sense that variance of the pointing movements could be reduced across trials. In other words, an indicator finger movement is planned, executed, and proprioceptive feedback in the indicator hand reveals that the finger did not land in the planned position. The brain could use this information to tune the motor command and make more accurate predictions of where the indicator finger will land. Importantly, this type of learning (a) does not involve the target hand, and (b) should occur similarly in both misaligned and veridical sessions. Consistent with this assumption, we found no evidence that finger variance improvement differed between the misaligned and veridical sessions. Importantly, the participant was always instructed to place their indicator finger where they perceived the target, and to make adjustments and take as much time as needed. When the indicator finger stopped moving, we therefore had to assume the participant felt it was placed at the target. At no time did the participant find out where the indicator finger actually landed in relation to the target, so there was no stimulus to drive any correction of errors in reaching the target.

A final consideration is whether intermanual transfer of any perceptual or motor changes could occur in a manner that might affect our conclusions. It is possible that any reductions in pointing variance in the indicator hand could transfer to the target hand, as improvements in other upper limb movement tasks are known to transfer intermanually (Yadav and Mutha 2020). However, both indicator hand improvements and transfer should occur equally in both sessions, so would not account for between-session differences in realignment-M1 excitability association. Based on the literature in visuomotor adaptation and proprioceptive realignment, it is unlikely that visuo-proprioceptive realignment in the target hand transferred to the indicator hand (Mostafa et al. 2014).

Determining any causal relationship between visuo-proprioceptive realignment and M1 excitability is beyond the scope of the present study. However, our findings are consistent with the involvement of M1 in high-level multisensory perception of the body. There is ample evidence of proprioceptive responses in M1 from illusory movement experiments (Hatsopoulos and Suminski 2011; Naito 2004), and some evidence of mirror neurons in M1, indicating visual responses (Hatsopoulos and

Suminski 2011). Hatsopoulos and Suminski (2011) note substantial heterogeneity of response properties in M1, with neurons responding to various combinations of voluntary movement, passive movement, and visual replay. In addition, lesions of M1 have been linked to impaired kinesthesia (Naito et al. 2011), suggesting M1 may actually play a role in kinesthetic perception (Hatsopoulos and Suminski 2011). Sensory activity in M1 could also reflect sensory guidance of movement (Ebbesen et al. 2018) or even predictions of the sensory consequences of movement (Hatsopoulos and Suminski 2011). Future work will be needed to determine if M1 activity plays a causal role in visuo-proprioceptive realignment of hand position estimates, or if M1 activity simply reflects the visuo-proprioceptive body schema.

M1 representation of other muscles did not show the same pattern

Modality-specific associations with M1 excitability were somatotopically focal. Like FDI, ADM excitability was negatively associated with proprioceptive realignment in the misaligned session. The ADM association with visual realignment, while positive like FDI, was not statistically significant. This is possible, despite the inverse relationship between (raw) visual and proprioceptive realignment, because the model relationships are what we have after controlling for the other sensory modality. Thus, the borderline-significant relationship with visual realignment for FDI, and no relationship with visual realignment for ADM, may indicate that the changes we measured in motor cortex have more to do with proprioceptive realignment, and only a little to do with visual realignment. Further studies will be needed to confirm this possibility. For example, repetitive TMS could be used to reduce excitability in somatosensory vs. visual cortex; based on the present results, we might predict a greater impact on visuo-proprioceptive realignment from somatosensory stimulation.

In a demographically similar group of healthy young adults, FCR, ECR, and BB showed no significant associations in the misaligned session. In other words, the pattern of associations observed for the misaligned index finger was partially present for the little finger, but absent for the more proximal muscles, apparently diminishing with distance from the misaligned finger. This suggests that visuo-proprioceptive realignment has localized neurophysiological effects, not broadly generalized to motor representations of body parts involved in moving the misaligned target finger. While the present study is the first, to our knowledge, to test M1 representations in the context of multisensory perceptual learning, our somatotopically focal results are consistent with the effects of peripheral somatosensory stimulation on M1. For example, vibration of one muscle increases M1 excitability for that muscle, but decreases it for neighboring muscles (Rosenkranz and Rothwell 2004).

TMS measures in proximal muscles are more variable than in distal muscles (Brasil-Neto et al. 1992; Harris-Love et al. 2007; Sankarasubramanian et al. 2015). However, others have found significant changes in proximal I/O curve areas after interventions such as ballistic wrist flexion practice (Ruddy et al. 2016) and paired associative stimulation (Carson et al. 2013). Indeed, Carson et al. (2013) used 6 TMS pulses per intensity while we used 15, to better control for variability in proximal responses and for variability linked to non-optimal targeting (i.e., targeting FCR for the BB I/O curve) (Brasil-Neto et al. 1992). Biceps responses were consistent with others who targeted the FCR hotspot (Carson et al. 2013), but small amplitudes pre-alignment task raise the possibility of a floor effect. In other words, perhaps participants who might otherwise have shown a decrease in BB excitability (i.e., realigned proprioception a lot, if the FDI pattern is followed) started out with such low BB responses that no reduction could be detected. However, of the two participants whose pre-misalignment biceps responses were on the low end of results in (Carson et al. 2013), neither had a high proprioceptive realignment magnitude. Therefore, a floor effect is unlikely to be a factor in the biceps results. In any case, all three arm muscles had an increase in excitability after the alignment task, regardless of session, suggesting the measure was sensitive enough to detect change. In addition, area under the I/O curve at baseline, and visual and proprioceptive estimates at baseline, were each correlated across sessions. The large effect sizes (Cohen 1992) are consistent with good between-session reliability of these measures. The absence of significant associations between realignment and M1 excitability in FCR, ECR, and BB is therefore unlikely to result from lack of measurement reliability.

Perceptual changes are also somatotopically focal

In Experiment 3, we found that changes in conscious perception of index fingertip position were closely related to proprioceptive estimates of the knuckle (first MP joint), but not the wrist or elbow. In other words, distortion in the body's representation was localized: If the index finger and knuckle felt like they were further away, perception of wrist and elbow positions did not change to match. This could reflect the brain striving to minimize distortion in the body representation (Butz et al. 2014), or perhaps it reflects mechanical and functional coupling between the first MP joint and the index fingertip, which does not exist to the same extent between the fingertip and the other joints tested.

Although these results are consistent with the somatotopically focal results in M1, some differences in the alignment task merit consideration. As we have done previously, the target finger in Experiments 1 and 2 was placed on one of two tactile markers beneath the glass for P and VP trials, and otherwise rested in the lap. Visuo-proprioceptive misalignment was 70 mm, and proprioceptive realignment at the fingertip was around 10 mm. Misalignment in Experiment 3 was only 35 mm, because we preserved the same rate of misalignment as well as the number of times participants were exposed to simultaneous visuo-proprioceptive information, at the expense of total misalignment magnitude. Even with only a 35 mm misalignment we might have expected proprioceptive realignment at the fingertip to be around 5 mm. Instead, it averaged only 2 mm. This is likely due to static positioning of the target arm, which rested fingertips-to-elbow on top of the glass throughout the task and was tied in place. Thus, participants had substantial tactile feedback telling them nothing was moving forward, contradicting the visual information. An additional limitation of this approach is that visual realignment cannot be assessed if the target arm (proprioception) is not removed from the workspace. It is possible, however, that greater realignment at the wrist and elbow would be observed if we were to increase the misalignment rate or number of trials to reach 70 mm misalignment. It is interesting that mean fingertip realignment was about equidistant between knuckle and elbow, and yet only correlated with knuckle. The forward realignment at the elbow (on average) is difficult to interpret from this experiment; it could be related to being furthest away from eye position (red cross). Further study of this paradigm, perhaps with other target arm configurations and measurement of visual estimates, could improve our understanding of the changes in body perception associated with visuo-proprioceptive realignment.

Implications for sensorimotor function

Our findings of somatotopically-focal effects of visuo-proprioceptive realignment on both motor neurophysiology and body perception are consistent with a tight relationship between sensory and motor systems. The effects of motor learning on sensory neurophysiology (Mirdamadi and Block 2020; Nasir et al. 2013; Vahdat et al. 2011) and perception (Henriques and Cressman 2012; Ostry et al. 2010; Salomonczyk et al. 2012; Wong et al. 2012) have been studied in some detail, at least with regard to proprioception. However, the specific effects of perceptual learning on the motor system have rarely been examined directly. Existing examples include work showing that somatosensory training affects functional connectivity with frontal motor regions (Rosenkranz and Rothwell 2012; Vahdat et al. 2014). The present study builds on this literature by examining the somatotopic effects of a multisensory perturbation on both M1 neurophysiology and body perception.

Our findings raise the possibility that perceptual learning may not generalize within a limb. Rather, visuo-proprioceptive misalignment appears to create a localized distortion in the multisensory body representation, with correspondingly local changes in the motor cortex representation. In contrast, motor skill learning is thought to involve a somewhat abstract control policy that can be applied with different effectors or limb segments. For example, the pattern of writing with the dominant hand is similar to writing with the non-dominant hand or feet (Schmidt and Lee 2011). Consistent with this idea, Rajan et al. (2019) found that a force production skill learned with the hand transferred to performance with the arm, and vice versa. While motor learning in general has been found to transfer symmetrically within a limb, trial-and-error motor adaptation transfers preferentially from proximal to distal effectors (Krakauer et al. 2006). Our present results suggest that visuo-proprioceptive realignment does not transfer from distal to proximal limb segments, as motor skill does. Further studies will be needed to determine if visuo-proprioceptive realignment at a proximal segment transfers distally.

While sensory processing and learning are critical for motor control, motor rehabilitation research has focused on motor, but not usually sensory, considerations of somatotopy. Proximal muscles are often the target for motor rehabilitation (Basteris et al. 2014; Prange et al. 2006), which might be expected to benefit hand function because of high overlap among M1 representations (Cunningham et al. 2013) and within-limb transfer of motor learning (Rajan et al. 2019). Because multisensory integration occurs by multiple parallel cortical and subcortical processes, it is spared in many clinical populations (Bolognini et al. 2015); this has raised interest in using multisensory exposure after stroke to facilitate motor recovery (Pazzaglia and Galli 2015; Rode et al. 2003). Existing multisensory upper limb motor rehabilitation techniques, such as virtual reality (Ekman et al. 2018; Keshner and Fung 2017), mirror training (Bolognini et al. 2015), action observation (Pazzaglia and Galli 2015), motor imagery (Johansson 2012), and robotic devices (Vanoglio et al. 2017) generally deal with the whole limb or upper body. If visuo-proprioceptive learning is somatotopically localized, as suggested by our results, it may be advantageous to adapt such techniques to include somatotopically focal training.

Conclusions

Here we examined the effect of a somatotopically localized visuo-proprioceptive mismatch on motor neurophysiology and conscious perception. We found somatotopically-focal effects in both domains. This correspondence highlights the tight relationship between sensory and motor systems, but also raises the possibility that perceptual learning may not generalize within the limb as motor skill learning does. Rather, it appears to create a localized distortion in the multisensory body representation, with correspondingly local changes in the motor cortex representation.

Funding: This work was supported by the National Science Foundation (grant number 1753915).

Acknowledgements: The authors would like to acknowledge Dr. Felipe Munoz-Rubke and Ms. Stephanie Dickinson for their advice on the statistical analysis of Experiments 1 and 2.

References

Andersen RA, **Snyder LH**, **Bradley DC**, **Xing J**. Multimodal representation of space in the posterior parietal cortex and its use in planning movements. *AnnuRevNeurosci* 20: 303–330, 1997.

Baizer JS, **Kralj-Hans I**, **Glickstein M**. Cerebellar lesions and prism adaptation in macaque monkeys. *J Neurophysiol* 81: 1960–1965, 1999.

Balslev D, **Nielsen FA**, **Lund TE**, **Law I**, **Paulson OB**. Similar brain networks for detecting visuo-motor and visuo-proprioceptive synchrony. *NeuroImage* 31: 308–312, 2006.

Basteris A, **Nijenhuis SM**, **Stienen AHA**, **Buurke JH**, **Prange GB**, **Amirabdollahian F**. Training modalities in robot-mediated upper limb rehabilitation in stroke: a framework for classification based on a systematic review. *J Neuroengineering Rehabil* 11: 111, 2014.

Bastian AJ. Learning to predict the future: the cerebellum adapts feedforward movement control. *CurrOpinNeurobiol* 16: 645–649, 2006.

Bates D, **Machler M**, **Bolker B**, **Walker S**. Fitting Linear Mixed-Effects Models Using lme4. *J Stat Softw* 67: 1:48, 2015.

van Beers RJ, **Sittig AC**, **Denier van der Gon JJ**. How humans combine simultaneous proprioceptive and visual position information. *ExpBrain Res* 111: 253–261, 1996.

van Beers RJ, **Sittig AC**, **Gon JJ**. Integration of proprioceptive and visual position-information: An experimentally supported model. *J Neurophysiol* 81: 1355–1364, 1999.

van Beers RJ, **Wolpert DM**, **Haggard P**. When feeling is more important than seeing in sensorimotor adaptation. *CurrBiol* 12: 834–837, 2002.

Block H, **Bastian A**, **Celnik P**. Virtual lesion of angular gyrus disrupts the relationship between visuoproprioceptive weighting and realignment. *J Cogn Neurosci* 25: 636–648, 2013.

Block H, **Celnik P**. Stimulating the cerebellum affects visuomotor adaptation but not intermanual transfer of learning. *Cerebellum Lond Engl* 12: 781–793, 2013.

Block HJ, **Bastian AJ**. Sensory reweighting in targeted reaching: effects of conscious effort, error history, and target salience. *JNeurophysiol* 103: 206–217, 2010.

Block HJ, **Bastian AJ**. Sensory weighting and realignment: independent compensatory processes. *JNeurophysiol* 106: 59–70, 2011.

Block HJ, **Bastian AJ**. Cerebellar involvement in motor but not sensory adaptation. *Neuropsychologia* 50: 1766–1775, 2012.

Block HJ, **Sexton BM**. Visuo-Proprioceptive Control of the Hand in Older Adults. *Multisensory Res* 34: 93–111, 2020.

Bolognini N, **Russo C**, **Vallar G**. Crossmodal illusions in neurorehabilitation. *Front Behav Neurosci* 9: 212, 2015.

Botvinick M, **Cohen J**. Rubber hands "feel" touch that eyes see. *Nature* 391: 756, 1998.

Brasil-Neto JP, **McShane LM**, **Fuhr P**, **Hallett M**, **Cohen LG**. Topographic mapping of the human motor cortex with magnetic stimulation: factors affecting accuracy and reproducibility. *Electroencephalogr Clin Neurophysiol* 85: 9–16, 1992.

Butz MV, **Kutter EF**, **Lorenz C**. Rubber hand illusion affects joint angle perception. *PloS One* 9: e92854, 2014.

Caligiore D, **Arbib MA**, **Miall RC**, **Baldassarre G**. The super-learning hypothesis: Integrating learning processes across cortex, cerebellum and basal ganglia. *Neurosci Biobehav Rev* 100: 19–34, 2019.

Carel C, **Loubinoux I**, **Boulanouar K**, **Manelfe C**, **Rascol O**, **Celsis P**, **Chollet F**. Neural Substrate for the Effects of Passive Training on Sensorimotor Cortical Representation: A Study with Functional Magnetic Resonance Imaging in Healthy Subjects. *J Cereb Blood Flow Metab* 20: 478–484, 2000.

Carson RG, **Nelson BD**, **Buick AR**, **Carroll TJ**, **Kennedy NC**, **Cann RM**. Characterizing Changes in the Excitability of Corticospinal Projections to Proximal Muscles of the Upper Limb. *Brain Stimul Basic Transl Clin Res Neuromodulation* 6: 760–768, 2013.

Clayton HA, **Cressman EK**, **Henriques DYP**. The effect of visuomotor adaptation on proprioceptive localization: the contributions of perceptual and motor changes. *Exp Brain Res* 1–14, 2014.

Cohen J. A power primer. *Psychol Bull* 112: 155–159, 1992.

Cook RD, **Weisberg S**. *Residuals and Influence in Regression*. 1st edition. New York: Springer, 1982.

Cressman EK, **Henriques DY**. Sensory recalibration of hand position following visuomotor adaptation. *J Neurophysiol* 102: 3505–3518, 2009.

Cunningham DA, **Machado A**, **Yue GH**, **Carey JR**, **Plow EB**. Functional somatotopy revealed across multiple cortical regions using a model of complex motor task. *Brain Res* 1531: 25–36, 2013.

Daniel Lüdecke. Data Visualization for Statistics in Social Science — sjPlot-package [Online]. https://CRAN.R-project.org/package=sjPlot [11 Apr. 2021].

Ebbesen CL, **Insanally MN**, **Kopec CD**, **Murakami M**, **Saiki A**, **Erlich JC**. More than Just a "Motor": Recent Surprises from the Frontal Cortex. *J Neurosci Off J Soc Neurosci* 38: 9402–9413, 2018.

Ekman U, **Fordell H**, **Eriksson J**, **Lenfeldt N**, **Wåhlin A**, **Eklund A**, **Malm J**. Increase of frontal neuronal activity in chronic neglect after training in virtual reality. *Acta Neurol Scand* 138: 284–292, 2018.

Ernst MO, **Banks MS**. Humans integrate visual and haptic information in a statistically optimal fashion. *Nature* 415: 429–433, 2002.

Galea JM, **Vazquez A**, **Pasricha N**, **Orban de**, **Celnik P**. Dissociating the Roles of the Cerebellum and Motor Cortex during Adaptive Learning: The Motor Cortex Retains What the Cerebellum Learns. *CerebCortex* 21: 1761–1770, 2011.

Ghahramani Z, **Wolpert DM**, **Jordan MI**. Computational models for sensorimotor integration. In: *Self-Organization, Computational Maps and Motor Control*, edited by Morasso PG, Sanguineti V. Amsterdam: North-Holland, 1997, p. 117–147.

Hagura N, **Oouchida Y**, **Aramaki Y**, **Okada T**, **Matsumura M**, **Sadato N**, **Naito E**. Visuokinesthetic perception of hand movement is mediated by cerebro-cerebellar interaction between the left cerebellum and right parietal cortex. *CerebCortex* 19: 176–186, 2009.

Hagura N, **Takei T**, **Hirose S**, **Aramaki Y**, **Matsumura M**, **Sadato N**, **Naito E**. Activity in the posterior parietal cortex mediates visual dominance over kinesthesia. *J Neurosci* 27: 7047–7053, 2007.

Harris C. Adaptation to displaced vision: visual, motor, or proprioceptive change? *Science* 140: 812–813, 1963.

Harris-Love ML, **Perez MA**, **Chen R**, **Cohen LG**. Interhemispheric Inhibition in Distal and Proximal Arm Representations in the Primary Motor Cortex. *J Neurophysiol* 97: 2511–2515, 2007.

Hatsopoulos NG, **Suminski AJ**. Sensing with the Motor Cortex. *Neuron* 72: 477–487, 2011.

Henriques DYP, **Cressman EK**. Visuomotor Adaptation and Proprioceptive Recalibration. *J Mot Behav* 44: 435–444, 2012.

Henriques DYP, **Medendorp WP**, **Gielen CC a. M**, **Crawford JD**. Geometric computations underlying eye-hand coordination: orientations of the two eyes and the head. *Exp Brain Res* 152: 70–78, 2003.

Johansson BB. Multisensory stimulation in stroke rehabilitation. *Front Hum Neurosci* 6: 60, 2012.

Kaernbach C, **Munka L**, **Cunningham D**. Visuomotor adaptation: Dependency on motion trajectory [Online]. In: *Dynamic Perception*. St. Augustin, p. 177–182. http://www.uni-kiel.de/psychologie/emotion/team/kaernbach/publications/2002_kae&al_bochum.pdf.

Keshner EA, **Fung J**. The quest to apply VR technology to rehabilitation: tribulations and treasures. *J Vestib Res Equilib Orientat* 27: 1–5, 2017.

Krakauer JW, **Mazzoni P**, **Ghazizadeh A**, **Ravindran R**, **Shadmehr R**. Generalization of motor learning depends on the history of prior action. *PLoSBiol* 4: e316, 2006.

Krubitzer LA, **Kaas JH**. The organization and connections of somatosensory cortex in marmosets. *J Neurosci* 10: 952–974, 1990.

Landi SM, **Baguear F**, **la-Maggiore V**. One week of motor adaptation induces structural changes in primary motor cortex that predict long-term memory one year later. *JNeurosci* 31: 11808–11813, 2011.

Lewis GN, **Byblow WD**. The effects of repetitive proprioceptive stimulation on corticomotor representation in intact and hemiplegic individuals. *Clin Neurophysiol Off J Int Fed Clin Neurophysiol* 115: 765–773, 2004.

Liu Y, **Sexton BM**, **Block HJ**. Spatial bias in estimating the position of visual and proprioceptive targets. *J Neurophysiol* , 2018. doi:10.1152/jn.00633.2017.

Martin TA, **Keating JG**, **Goodkin HP**, **Bastian AJ**, **Thach WT**. Throwing while looking through prisms. II. Specificity and storage of multiple gaze-throw calibrations. *Brain* 119 (Pt 4): 1199–1211, 1996.

McElreath R. *Statistical Rethinking: A Bayesian Course with Examples in R and Stan*. 1 edition. Boca Raton: Chapman and Hall/CRC, 2015.

Mirdamadi JL, **Block HJ**. Somatosensory changes associated with motor skill learning. *J Neurophysiol* 123: 1052–1062, 2020.

Mon-Williams M, **Wann JP**, **Jenkinson M**, **Rushton K**. Synaesthesia in the normal limb. *ProcBiolSci* 264: 1007–1010, 1997.

Mostafa AA, **'t Hart BM**, **Henriques DYP**. Motor learning without moving: Proprioceptive and predictive hand localization after passive visuoproprioceptive discrepancy training. *PloS One* 14: e0221861, 2019.

Mostafa AA, **Salomonczyk D**, **Cressman EK**, **Henriques DYP**. Intermanual transfer and proprioceptive recalibration following training with translated visual feedback of the hand. *Exp Brain Res* 232: 1639–1651, 2014.

Munoz-Rubke F, **Mirdamadi JL**, **Lynch AK**, **Block HJ**. Modality-specific Changes in Motor Cortex Excitability After Visuo-proprioceptive Realignment. *J Cogn Neurosci* 29: 2054–2067, 2017.

Naito E. Sensing limb movements in the motor cortex: how humans sense limb movement. *Neuroscientist* 10: 73–82, 2004.

Naito E, **Matsumoto R**, **Hagura N**, **Oouchida Y**, **Tomimoto H**, **Hanakawa T**. Importance of precentral motor regions in human kinesthesia: a single case study. *Neurocase* 17: 133–147, 2011.

Nasir SM, **Darainy M**, **Ostry DJ**. Sensorimotor adaptation changes the neural coding of somatosensory stimuli. *J Neurophysiol* 109: 2077–2085, 2013.

Nieuwenhuis R, **Grotenhuis M te**, **Pelzer B**. influence.ME: Tools for Detecting Influential Data in Mixed Effects Models. *R J* 4: 38–47, 2012.

Nourouzpour N, **Salomonczyk D**, **Cressman EK**, **Henriques DYP**. Retention of proprioceptive recalibration following visuomotor adaptation. *Exp Brain Res* 233: 1019–1029, 2015.

Ostry DJ, **Darainy M**, **Mattar AA**, **Wong J**, **Gribble PL**. Somatosensory plasticity and motor learning. *JNeurosci* 30: 5384–5393, 2010.

Ostry DJ, **Gribble PL**. Sensory Plasticity in Human Motor Learning. *Trends Neurosci* 39: 114–123, 2016.

Pazzaglia M, **Galli G**. Translating novel findings of perceptual-motor codes into the neuro-rehabilitation of movement disorders. *Front Behav Neurosci* 9: 222, 2015.

Prange GB, **Jannink MJA**, **Groothuis-Oudshoorn CGM**, **Hermens HJ**, **Ijzerman MJ**. Systematic review of the effect of robot-aided therapy on recovery of the hemiparetic arm after stroke. *J Rehabil Res Dev* 43: 171–184, 2006.

R Core Team. R: The R Project for Statistical Computing [Online]. R Foundation for Statistical Computing.https://www.r-project.org/ [5 Sep. 2016].

Rajan VA, **Hardwick RM**, **Celnik PA**. Reciprocal intralimb transfer of skilled isometric force production. *J Neurophysiol* 122: 60–65, 2019.

Rode G, **Pisella L**, **Rossetti Y**, **Farnè A**, **Boisson D**. Bottom-up transfer of sensory-motor plasticity to recovery of spatial cognition: visuomotor adaptation and spatial neglect. *Prog Brain Res* 142: 273–287, 2003.

Rosenkranz K, **Rothwell JC**. The effect of sensory input and attention on the sensorimotor organization of the hand area of the human motor cortex. *J Physiol* 561: 307–320, 2004.

Rosenkranz K, **Rothwell JC**. Modulation of proprioceptive integration in the motor cortex shapes human motor learning. *J Neurosci Off J Soc Neurosci* 32: 9000–9006, 2012.

Rossi C, **Bastian AJ**, **Therrien AS**. Mechanisms of proprioceptive realignment in human motor learning. *Curr Opin Physiol* 20: 186–197, 2021.

Rossi S, **Hallett M**, **Rossini PM**, **Pascual-Leone A**, **Safety of TMS Consensus Group**. Safety, ethical considerations, and application guidelines for the use of transcranial magnetic stimulation in clinical practice and research. *Clin Neurophysiol Off J Int Fed Clin Neurophysiol* 120: 2008–2039, 2009.

Rossini PM, **Burke D**, **Chen R**, **Cohen LG**, **Daskalakis Z**, **Di Iorio R**, **Di Lazzaro V**, **Ferreri F**, **Fitzgerald PB**, **George MS**, **Hallett M**, **Lefaucheur JP**, **Langguth B**, **Matsumoto H**, **Miniussi C**, **Nitsche MA**, **Pascual-Leone A**, **Paulus W**, **Rossi S**, **Rothwell JC**, **Siebner HR**, **Ugawa Y**, **Walsh V**, **Ziemann U**. Non-invasive electrical and magnetic stimulation of the brain, spinal cord, roots and peripheral nerves: Basic principles and procedures for routine clinical and research application. An updated report from an I.F.C.N. Committee. *Clin Neurophysiol Off J Int Fed Clin Neurophysiol* 126: 1071–1107, 2015.

Ruddy KL, **Rudolf AK**, **Kalkman B**, **King M**, **Daffertshofer A**, **Carroll TJ**, **Carson RG**. Neural Adaptations Associated with Interlimb Transfer in a Ballistic Wrist Flexion Task. *Front Hum Neurosci* 10, 2016.

Ruttle JE, **Cressman EK**, **'t Hart BM**, **Henriques DYP**. Time Course of Reach Adaptation and Proprioceptive Recalibration during Visuomotor Learning. *PLoS ONE* 11, 2016.

Ruttle JE, **'t Hart BM**, **Henriques DYP**. The fast contribution of visual-proprioceptive discrepancy to reach aftereffects and proprioceptive recalibration. *PloS One* 13: e0200621, 2018.

Sainburg RL. Evidence for a dynamic-dominance hypothesis of handedness. *Exp Brain Res* 142: 241–258, 2002.

Salomonczyk D, **Cressman EK**, **Henriques DYP**. The role of the cross-sensory error signal in visuomotor adaptation. *Exp Brain Res* 228: 313–325, 2013.

Salomonczyk D, **Henriques DYP**, **Cressman EK**. Proprioceptive recalibration in the right and left hands following abrupt visuomotor adaptation. *Exp Brain Res* 217: 187–196, 2012.

Sankarasubramanian V, **Roelle SM**, **Bonnett CE**, **Janini D**, **Varnerin NM**, **Cunningham DA**, **Sharma JS**, **Potter-Baker KA**, **Wang X**, **Yue GH**, **Plow EB**. Reproducibility of transcranial magnetic stimulation metrics in the study of proximal upper limb muscles. *J Electromyogr Kinesiol Off J Int Soc Electrophysiol Kinesiol* 25: 754–764, 2015.

Schlerf J, **Ivry RB**, **Diedrichsen J**. Encoding of sensory prediction errors in the human cerebellum. *J Neurosci Off J Soc Neurosci* 32: 4913–4922, 2012.

Schmidt RA, **Lee TD**. *Motor control and learning: a behavioral emphasis*. Leeds: Human Kinetics, 2011.

Shadmehr R, **Smith MA**, **Krakauer JW**. Error correction, sensory prediction, and adaptation in motor control. *Annu Rev Neurosci* 33: 89–108, 2010.

Shams L, **Kamitani Y**, **Shimojo S**. Illusions. What you see is what you hear. *Nature* 408: 788, 2000.

Sober SJ, **Sabes PN**. Flexible strategies for sensory integration during motor planning. *Nat Neurosci* 8: 490–497, 2005.

Strigaro G, **Ruge D**, **Chen J-C**, **Marshall L**, **Desikan M**, **Cantello R**, **Rothwell JC**. Interaction between visual and motor cortex: a transcranial magnetic stimulation study. *J Physiol* 593: 2365–2377, 2015.

Suzuki M, **Kirimoto H**, **Sugawara K**, **Watanabe M**, **Shimizu S**, **Ishizaka I**, **Yamada S**, **Matsunaga A**, **Fukuda M**, **Onishi H**. Induction of cortical plasticity for reciprocal muscles by paired associative stimulation. *Brain Behav* 4: 822–832, 2014.

Vahdat S, **Darainy M**, **Milner TE**, **Ostry DJ**. Functionally specific changes in resting-state sensorimotor networks after motor learning. *J Neurosci Off J Soc Neurosci* 31: 16907–16915, 2011.

Vahdat S, **Darainy M**, **Ostry DJ**. Structure of plasticity in human sensory and motor networks due to perceptual learning. *J Neurosci Off J Soc Neurosci* 34: 2451–2463, 2014.

Vanoglio F, **Bernocchi P**, **Mulè C**, **Garofali F**, **Mora C**, **Taveggia G**, **Scalvini S**, **Luisa A**. Feasibility and efficacy of a robotic device for hand rehabilitation in hemiplegic stroke patients: a randomized pilot controlled study. *Clin Rehabil* 31: 351–360, 2017.

Welch RB. Adaptation of space perception. New York: Wiley, 1986.

Welch RB, **Warren DH**. Immediate perceptual response to intersensory discrepancy. *PsycholBull* 88: 638–667, 1980.

Welch RB, **Widawski MH**, **Harrington J**, **Warren DH**. An examination of the relationship between visual capture and prism adaptation. *PerceptPsychophys* 25: 126–132, 1979.

Wong JD, **Kistemaker DA**, **Chin A**, **Gribble PL**. Can proprioceptive training improve motor learning? *J Neurophysiol* 108: 3313–3321, 2012.

Yadav G, **Mutha PK**. Symmetric interlimb transfer of newly acquired skilled movements. *J Neurophysiol* 124: 1364–1376, 2020.

Zbib B, **Henriques DYP**, **Cressman EK**. Proprioceptive recalibration arises slowly compared to reach adaptation. *Exp Brain Res* 234: 2201–2213, 2016.

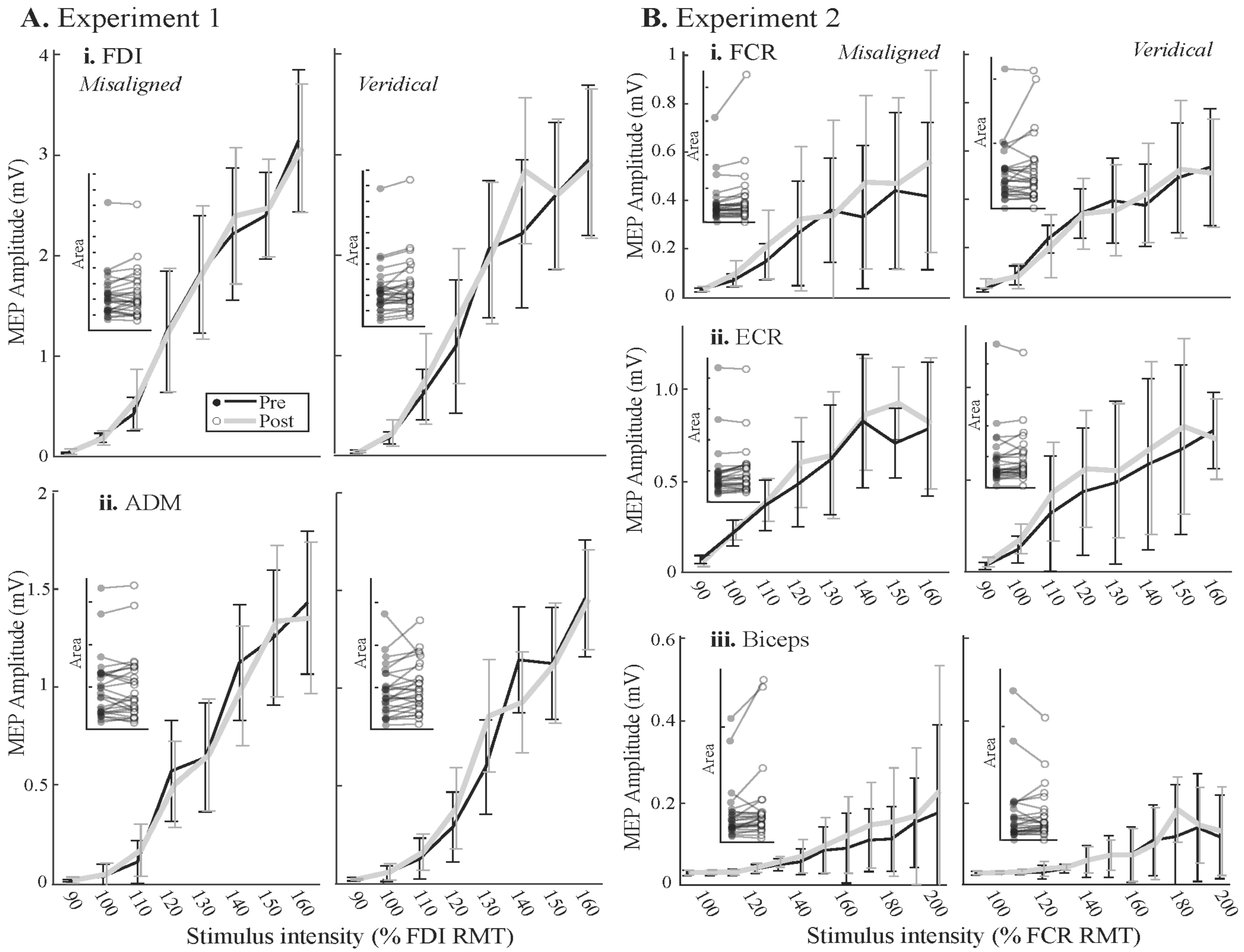

Figure S1. Experiment 1 **(A)** and 2 **(B)** input/output curves. Median MEP amplitudes arranged in order of increasing stimulus intensity, pre- and post-alignment task in the misaligned (black lines) and veridical (grey lines) sessions. Error bars represent 95% CI. **Insets:** individual participants' area under the input/output curves pre- and post-alignment task. Each notch on the y-axis represents an area of 50.

Table S1. Experiment 1 multilevel regression results for FDI muscle, comprising four interaction terms for session type (veridical or misaligned) and realignment type (proprioceptive or visual).

	FDI			
Predictors	*β(CI)*	t_{47}	*p*	*r*
Fixed parts				
Intercept	4.69 (4.60, 4.79)	95.78	**<0.001**	
Veridical session : Proprioceptive realignment	0.0016 (-0.0075, 0.0108)	0.35	0.723	0.002
Misaligned session : Proprioceptive realignment	-0.010 (-0.017, -0.003)	-2.85	**0.004**	-0.488
Veridical session : Visual realignment	-0.0040 (-0.013, 0.0049)	-0.89	0.375	-0.13
Misaligned session : Visual realignment	0.0037 (0.0000, 0.0073)	1.99	**0.047**	0.601
Random parts				
NID	27			
Observations	54			

Columns represent log-transformed percentage of baseline (post divided by pre) in area under the I/O curve. βs are presented with their 95% CIs. The test statistic (t) is calculated from the parameter estimate divided by SE, and p-values are calculated based on the t-statistic with corresponding degrees of freedom. Boldface identifies statistically significant results. Correlations between realignment residuals and log-transformed percentage of baseline area under the I/O curve were computed to provide an effect size for each parameter estimate, r.

Table S2. Experiment 1 multilevel regression results for ADM muscle, comprising four interaction terms for session type (veridical or misaligned) and realignment type (proprioceptive or visual).

	ADM			
Predictors	*β(CI)*	t_{47}	*p*	*r*
Fixed parts				
Intercept	4.74 (4.60, 4.89)	64.95	**<0.001**	
Veridical session : Proprioceptive realignment	-0.0005 (-0.014, 0.013)	-0.08	0.939	-0.077
Misaligned session : Proprioceptive realignment	-0.013 (-0.023, -0.002)	-2.43	**0.015**	-0.344
Veridical session : Visual realignment	-0.004 (-0.017, 0.009)	-0.62	0.534	-0.081
Misaligned session : Visual realignment	0.0022 (-0.0031, 0.0075)	0.81	0.418	0.406
Random parts				
NID	27			
Observations	54			

Columns represent log-transformed percentage of baseline (post divided by pre) in area under the I/O curve. βs are presented with their 95% CIs. The test statistic (t) is calculated from the parameter estimate divided by SE, and p-values are calculated based on the t-statistic with corresponding degrees of freedom. Boldface identifies statistically significant results. Correlations between realignment residuals and log-transformed percentage of baseline area under the I/O curve were computed to provide an effect size for each parameter estimate, r.

Table S3. Experiment 2 multilevel regression results for FCR muscle, comprising four interaction terms for session type (veridical or misaligned) and realignment type (proprioceptive or visual)

	FCR			
Predictors	*β(CI)*	t_{45}	*p*	*r*
Fixed parts				
Intercept	4.66 (4.55, 4.77)	84.15	**<0.001**	
Veridical session : Proprioceptive realignment	-0.0089 (-0.0202, 0.0024)	-1.54	0.124	-0.225
Misaligned session : Proprioceptive realignment	0.0022 (-0.0039, 0.0083)	0.70	0.483	0.124
Veridical session : Visual realignment	0.0092 (-0.0002, 0.0187)	1.92	0.055	0.248
Misaligned session : Visual realignment	0.0016 (-0.0013, 0.0045)	1.07	0.285	-0.231
Random parts				
N_{ID}	26			
Observations	52			

Columns represent log-transformed percentage of baseline (post divided by pre) in area under the I/O curve. βs are presented with their 95% CIs. The test statistic (t) is calculated from the parameter estimate divided by SE, and p-values are calculated based on the t-statistic with corresponding degrees of freedom. Boldface identifies statistically significant results. Correlations between realignment residuals and log-transformed percentage of baseline area under the I/O curve were computed to provide an effect size for each parameter estimate, r.

Table S4. Experiment 2 multilevel regression results for ECR muscle, comprising four interaction terms for session type (veridical or misaligned) and realignment type (proprioceptive or visual)

	ECR			
Predictors	*β(CI)*	t_{45}	*p*	*r*
Fixed parts				
Intercept	4.71 (4.63, 4.80)	103.54	**<0.001**	
Veridical session : Proprioceptive realignment	0.0073 (-0.0012, 0.0158)	1.68	0.093	0.235
Misaligned session : Proprioceptive realignment	0.0014 (-0.0034, 0.0061)	0.57	0.572	0.12
Veridical session : Visual realignment	0.0011 (-0.0062, 0.0083)	0.29	0.773	0.123
Misaligned session : Visual realignment	-0.0006 (-0.0027, 0.0015)	-0.56	0.577	-0.249
Random parts				
N_{ID}	26			
Observations	52			

Columns represent log-transformed percentage of baseline (post divided by pre) in area under the I/O curve. βs are presented with their 95% CIs. The test statistic (t) is calculated from the parameter estimate divided by SE, and p-values are calculated based on the t-statistic with corresponding degrees of freedom. Boldface identifies statistically significant results. Correlations between realignment residuals and log-transformed percentage of baseline area under the I/O curve were computed to provide an effect size for each parameter estimate, r.

Table S5. Experiment 2 multilevel regression results for BB muscle, comprising four interaction terms for session type (veridical or misaligned) and realignment type (proprioceptive or visual)

	BB			
Predictors	*β(CI)*	t_{45}	*p*	*r*
Fixed parts				
Intercept	4.75 (4.61, 4.89)	67.42	**<0.001**	
Veridical session : Proprioceptive realignment	0.0039 (-0.0112, 0.0190)	0.50	0.615	0.054
Misaligned session : Proprioceptive realignment	0.0023 (-0.0057, 0.0104)	0.57	0.57	0.059
Veridical session : Visual realignment	-0.0038 (-0.0162, 0.0087)	-0.59	0.555	0.051
Misaligned session : Visual realignment	-0.0007 (-0.0048, 0.0034)	-0.34	0.737	-0.25
Random parts				
N_{ID}	26			
Observations	52			

Columns represent log-transformed percentage of baseline (post divided by pre) in area under the I/O curve. βs are presented with their 95% CIs. The test statistic (t) is calculated from the parameter estimate divided by SE, and p-values are calculated based on the t-statistic with corresponding degrees of freedom. Boldface identifies statistically significant results. Correlations between realignment residuals and log-transformed percentage of baseline area under the I/O curve were computed to provide an effect size for each parameter estimate, r.